Development 138, 2793-2805 (2011) doi:10.1242/dev.063644

A context-dependent combination of Wnt receptors controls axis elongation and leg development in a short germ insect

Anke Beermann[1,2,*], Romy Prühs[1], Rebekka Lutz[1,2] and Reinhard Schröder[1,*]

SUMMARY

Short germ embryos elongate their primary body axis by consecutively adding segments from a posteriorly located growth zone. Wnt signalling is required for axis elongation in short germ arthropods, including *Tribolium castaneum*, but the precise functions of the different Wnt receptors involved in this process are unclear. We analysed the individual and combinatorial functions of the three Wnt receptors, Frizzled-1 (Tc-Fz1), Frizzled-2 (Tc-Fz2) and Frizzled-4 (Tc-Fz4), and their co-receptor Arrow (Tc-Arr) in the beetle *Tribolium*. Knockdown of gene function and expression analyses revealed that Frizzled-dependent Wnt signalling occurs anteriorly in the growth zone in the presegmental region (PSR). We show that simultaneous functional knockdown of the Wnt receptors *Tc-fz1* and *Tc-fz2* via RNAi resulted in collapse of the growth zone and impairment of embryonic axis elongation. Although posterior cells of the growth zone were not completely abolished, Wnt signalling within the PSR controls axial elongation at the level of pair-rule patterning, Wnt5 signalling and FGF signalling. These results identify the PSR in *Tribolium* as an integral tissue required for the axial elongation process, reminiscent of the presomitic mesoderm in vertebrates. Knockdown of *Tc-fz1* alone interfered with the formation of the proximo-distal and the dorso-ventral axes during leg development, whereas no effect was observed with single *Tc-fz2* or *Tc-fz4* RNAi knockdowns. We identify *Tc-Arr* as an obligatory Wnt co-receptor for axis elongation, leg distalisation and segmentation. We discuss how Wnt signalling is regulated at the receptor and co-receptor levels in a dose-dependent fashion.

KEY WORDS: Wnt signalling, Frizzled receptors, Axis elongation, Short germ embryogenesis, *Tribolium*

INTRODUCTION

The precise regulation of cell-cell communication through signalling pathways is essential for both embryogenesis and organogenesis. One significant pathway is the evolutionarily conserved Wnt signalling pathway (Janssen et al., 2010), which coordinates crucial cellular processes such as proliferation, polarity, migration, and the determination of cell fate (Habas and Dawid, 2005; Logan and Nusse, 2004; Widelitz, 2005).

The canonical or β-catenin-dependent Wnt pathway is initiated by the binding of the Wnt ligand to transmembrane receptors encoded by the Frizzled gene family. This action causes β-catenin to be stabilised in the cytoplasm and translocated into the nucleus where it activates the transcription of target genes (Bhanot et al., 1996; Cadigan and Nusse, 1997; Chen and Struhl, 1999; Hsieh et al., 1999; Rulifson et al., 2000; Wu et al., 2004; Yang-Snyder et al., 1996). Proteins of the low-density-lipoprotein (LDL) receptor-related (LRP) class act as Wnt co-receptors; in insects, they are represented by the *Drosophila* LDL-receptor Arrow (Wehrli et al., 2000) and in vertebrates by LRP5 and LRP6 (Pinson et al., 2000; Tamai et al., 2000).

Vertebrate and arthropod embryos rapidly elongate their body axes during early embryogenesis by adding body segments during a post-blastodermal growth phase. The central tissue controlling axial elongation (AE) is a proliferative zone at the posterior of the embryo known as the growth zone or, more generally, as the segment addition zone (Janssen et al., 2010). In arthropods, this part of the embryo is defined as the region immediately posterior to the last generated segment, the presegmental region (PSR) and the paddle-shaped posterior growth zone (Martin and Kimelman, 2009; Schröder et al., 2008). In vertebrates, the presomitic mesoderm (PSM) sheds blocks of mesodermal tissue, the somites, under the control of graded fibroblast growth factor (FGF) and Wnt signalling pathways (Aulehla et al., 2008; Dequéant and Pourquié, 2008). In arthropods, key molecules, such as *caudal* and *torso*/*torsolike*, as well as the Wnt ligand Wnt8 and other Wnt pathway members (*armadillo*/β-catenin, *pangolin*/TCF and *arrow*/LRP5/6) are required for setting up the growth zone and maintaining axis elongation (Bolognesi et al., 2008b; Bolognesi et al., 2009; Copf et al., 2004; McGregor et al., 2008; Miyawaki et al., 2004). Body axis elongation cannot be studied in *Drosophila* because all segments form almost simultaneously (long germ embryogenesis). Recent functional studies have demonstrated the involvement of *Tribolium arrow* and *Tc-Wnt 8/D* in axis formation (Bolognesi et al., 2008b; Bolognesi et al., 2009). Because only strong $arrow^{RNAi}$ phenotypes have been analysed, the complex role of the Wnt co-receptor has only been partially resolved. How *Tribolium* generates cellular complexity at the Wnt receptor level is not known.

In this paper, we investigated the role of Wnt receptor genes (*Tc-fz1*, *Tc-fz2* and *Tc-fz4*) and the co-receptor gene (*Tc-arrow*) in different processes of *Tribolium* embryogenesis. We first characterised Wnt-receptive sites in the *Tribolium* embryo by analysing the expression patterns of the Wnt receptors. We found that, as in *Drosophila* (Kennerdell and Carthew, 1998), the Wnt receptors Tc-Fz1 and Tc-Fz2 function redundantly. In *Tribolium*, they are necessary for the maintenance of a functional growth zone.

[1]Universität Rostock, Institut für Biowissenschaften/Abt. Genetik, D-18059 Rostock, Germany. [2]Interfakultäres Institut für Zellbiologie, Abt. Genetik der Tiere, Auf der Morgenstelle 28, D-72076 Tübingen, Germany.

*Authors for correspondence (beermann@uni-tuebingen.de; reinhard.schroeder@uni-rostock.de)

Accepted 6 April 2011

In *Tc-fz-1/2*^{RNAi} embryos, axis elongation stops prematurely. In the collapsed growth zone of *Tc-fz-1/2*^{RNAi} embryos, posterior cells are still present, but the transition from pair-rule to the segmental function of Even-skipped is impaired. *Tc-frizzled 1* plays a *Tc-frizzled 2*-independent role in leg formation, whereas *Tc-frizzled 4* supports *Tc-fz1* in leg development and additionally functions in gut development. We identify Tc-Arrow as the obligatory Wnt co-receptor for Wnt-dependent processes, complementing previous studies (Bolognesi et al., 2009). Finally, we discuss the dosage dependency of Wnt receptor-co-receptor interactions in body and leg axis development.

MATERIALS AND METHODS

Gene identification

LRP, *frizzled* and *arrow* gene homologues in the *Tribolium* genome (http://beetlebase.org) (Kim et al., 2010) were identified using BLAST with the *Drosophila* protein sequences. Sequence analysis, sequence alignment and PCR primer design were performed using the programs Edit Seq, MegAlign and Primer Select from the Lasergene DNASTAR package. The phylogenetic relationship of the protein sequences was based on a Clustal-W alignment and analysed with TREE-PUZZLE (Strimmer and von Haeseler, 1996). The trees in Fig. 1 were visualised with TreeView (Page, 1996) and Dendroscope (Huson et al., 2007).

The following amino acid sequences were used for the alignment in Fig. 1 [protein (species) Accession Number (amino acid positions)].

Frizzled-1/7

DmFz1 (*Drosophila melanogaster*) CAA38458 (1>581); AgFz1 (*Anopheles gambiae*) XP_317942 (1>181); TcFz1 (*Tribolium castaneum*) NP_001164247/TC014055 (1>549); NasFz7 (*Nasonia vitripennis*) XP_001605802 (1>580); DrFz7a (*Danio rerio*) AAH68322 (1>559); DrFz7b (*Danio rerio*) NP_739569 (1>557); MmFz7 (*Mus musculus*) AAH49781 (1>750); XenFz7 (*Xenopus laevis*) AAF63152 (1>549).

Frizzled-2/5/8

DmFz2 (*Drosophila melanogaster*) AAC47273 (1>694); TcFz2 (*Tribolium castaneum*) EFA01325/TC003407 (1>605); DrFz5 (*Danio rerio*) NP_571209 (1>592); DrFz8 (*Danio rerio*) NP_570993 (1>579); MmFz5 (*Mus musculus*) NP_073558 (1>585); MmFz8 (*Mus musculus*) NP_032084 (1>685); AgFz2 (*Anopheles gambiae*) XP_311505 (1>687).

Frizzled-3

DmFz3 (*Drosophila melanogaster*) ABW09320 (1>646); NasFz3 (*Nasonia vitripennis*) XP_001600300 (1>573); AgFz3 (*Anopheles gambiae*) XP_310970 (1>487).

Frizzled-4

TcFz4 (*Tribolium castaneum*) EFA09255/TC006527 (1>527); DmFz4 (*Drosophila melanogaster*) NP_511068 (1>705); AgFz4 (*Anopheles gambiae*) XP_319612 (1>580); MmFz4 (*Mus musculus*) NP_032081 (1>537).

Frizzled 9/10

DrFz10 (*Danio rerio*) AAH76546 (1>580); MmFz9 (*Mus musculus*) AAB87503 (1>549); MmFz10 (*Mus musculus*) NP_780493 (1>582).

Arrow/LRP5/LRP6

TcArr (*Tribolium castaneum*) XP_975483/ TC008151 (1>1580); DmArr (*Drosophila melanogaster*) NP_524737 (1>1678); AgArr (*Anopheles gambiae*) XP_320740 (1>1619); NasArr (*Nasonia vitripennis*) XP_001603043 (1>1634); DrLRP5 (*Danio rerio*) XP_696943 (1>1593); DrLRP6 (*Danio rerio*) NP_001128156 (1>1620); MmLRP5 (*Mus musculus*) NP_032539 (1>1614); MmLRP6 (*Mus musculus*) NP_032540 (1>1613).

LRP4

TcLRP4 (*Tribolium castaneum*) XP_001814959/ TC007146 (1>2041); DmLRP4 (*Drosophila melanogaster*) NP_727914 (1>2009); AgLRP4 (*Anopheles gambiae*) XP_311125 (1>1740); NasLRP4 (*Nasonia vitripennis*) XP_001605666 (1>2084); DrLRP4 (*Danio rerio*) XP_697930 (1>1243); MmLRP4 (*Mus musculus*) EDL27564 (1>1911).

The following gene fragments were cloned and used for in situ hybridisation and dsRNA production: *Tc-fz1* (accession number: NM_001170776), an 881-bp fragment corresponding to position 127-1007; *Tc-fz2* (XM_963025/867-bp fragment, position 81-947); *Tc-fz4* (XM_962510, 534 bp, position 822-1355), *Tc-arrow* (XM 970390, 694 bp, position 1712-2413). These fragments show no sequence identity of longer than 19 consecutive nucleotides within the predicted coding region of the *Tribolium* genome that could serve as off-targets in RNA interference. In the case of *Tc-fz1*, a 21-bp identity exists with a non-coding genomic region. Cross-reactivity of *fz1* and *fz2* was not expected because the two genes contain only short sequences of identity (12 bp). This prediction was borne out by the non-overlapping results obtained in the respective single RNAi experiments.

Molecular biology

cDNA was synthesised from total RNA (RNeasy/Qiagen) using random hexamer primers from the Transcriptor First Strand cDNA Synthesis Kit (Roche). PCR fragments were subcloned into the pCR4 vector of the TOPO-TA Cloning Kit (Invitrogen) and sequenced by AGOWA (Berlin). Double-stranded RNA for RNA interference was produced with the MEGAscript in vitro transcription kit (Ambion) and injected into pupae or adults (parental RNAi) at several different concentrations in multiple independent experiments (see Table S1B1-6 in the supplementary material) under standard conditions (Bucher et al., 2002; Schröder et al., 2008).

The parental application of dsRNA results in the knockdown of both the maternal and zygotic transcripts; the effect is most strongly seen in the first egglays from the treated females and diminishes with successive egglays. In this way, a variety of phenotypes ('phenotypic series') were achieved, and weaker phenotypes were explained by a lower dose of dsRNA in the respective embryo. The absence of the *Tc-fz2*-RNA transcript has been confirmed by in situ hybridisation in *Tc-fz1/2*^{RNAi} embryos (see Fig. S3 in the supplementary material).

All other molecular techniques were performed according to the instructions of the suppliers or following standard protocols (Sambrook et al., 1989).

Analysis of embryos and larvae

Fixation of embryos and cuticle preparations of first instar larvae were performed as previously described (Patel, 1994; Van der Meer, 1977). In situ hybridisation to RNA transcripts was performed as published (Tautz and Pfeifle, 1989). Embryos were embedded in 100% glycerol and photographed on an Axiophot Zeiss microscope. Immunolocalisation studies of the Even-skipped and Engrailed proteins were performed as previously described (Patel et al., 1994) using the respective monoclonal antibodies at a dilution of 1:100 obtained from the Developmental Studies Hybridoma Bank.

Animal husbandry

Wild-type beetles of the San Bernardino strain were reared on whole-wheat flour in a 30°C incubator; the collection of eggs and pupae was performed as previously described (Beermann et al., 2004).

RESULTS

Conservation of Wnt signal perception in *Tribolium*

Three frizzled genes and one arrow orthologue coding for Wnt receptors and a Wnt co-receptor, respectively, are present in the *Tribolium* genome (Fig. 1). Our phylogenetic analysis grouped the Tc-Frizzled proteins together with other insect and vertebrate Frizzled proteins into three subfamilies (Fig. 1A). Tc-Frizzled-1, the orthologue of *Drosophila* Frizzled, clusters with other arthropod Frizzled-1 proteins and vertebrate Frizzled-7 proteins within the Frizzled-1/7 subfamily. The insect Frizzled-2 proteins and the vertebrate Frizzled-5 and Frizzled-8 proteins constitute the Frizzled-

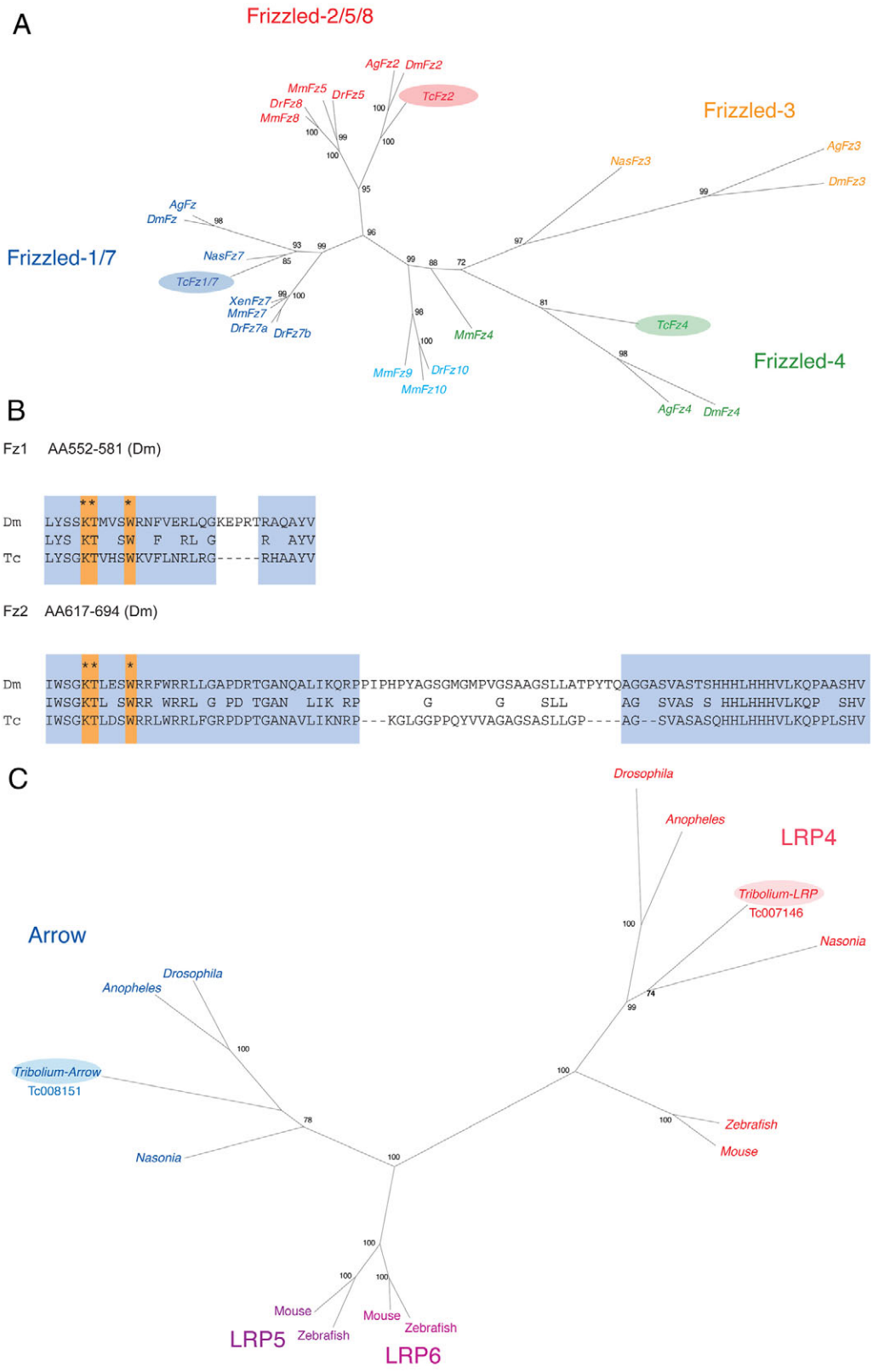

Fig. 1. Three Frizzled and two Arrow/LRP proteins are encoded in the *Tribolium* genome. (**A**) Phylogenetic analysis places the Tc-Frizzled protein-sequences within three Frizzled classes: 1/7, 2/5/8 and 3/4/9/10. No *Tribolium* representative of the frizzled-3 gene family was found. (**B**) Sequence alignment of the C-terminus of the *Drosophila* and *Tribolium* Frizzled-1 and Frizzled-2 proteins. Both *Tribolium* Fz proteins share the specific binding sites for the protein Dishevelled (Wu and Mlodzik, 2008). Blue indicates conserved regions. Orange and asterisks indicate conserved binding sites. Dm, *Drosophila melanogaster*; Tc, *Tribolium castaneum*. (**C**) Phylogenetic analysis of the *Tribolium* Arrow and LRP proteins.

2/5/8 subfamily. Frizzled-4 together with dipteran and vertebrate Frizzled-4 orthologues and the vertebrate Frizzled-10 proteins represent the third group. The significant amino acids necessary for binding Dishevelled (Umbhauer et al., 2000; Wu and Mlodzik, 2008) are conserved in the Frizzled C-terminal regions (Fig. 1B), reinforcing the classification of the *Tribolium* Frizzled proteins.

A single *Tribolium* Wnt co-receptor of the Arrow/LRP class

Within the *Tribolium* genome, the single orthologue of the *Drosophila* Wnt co-receptor Arrow is encoded by *Tc-arrow* (Tc008151). Another gene coding for a protein with the low-density-lipid (LDL) receptor related protein (LRP) motif was identified as the *Tribolium* LRP4 protein (Tc007146; Fig. 1C). However, only Tc-Arrow contains the multiple phosphorylation sites for Axin and Gsk3β in its cytoplasmic part, suggesting that Tc-Arrow has a similar functional role as *Drosophila* Arrow in Wnt signalling (see Fig. S4 in the supplementary material).

Tc-frizzled-2 and *Tc-frizzled-4*, but not *Tc-frizzled-1* or *Tc-arrow*, show distinct temporal and spatial expression patterns

Tc-fz-2 expression started at the early blastoderm stage at which point it covered the prospective head region for 53-82% of the egg length (100%=anterior pole). Dorsally, the head-specific domain was narrower than at the ventral side (Fig. 2A,A′, bars). When the germ rudiment became visible, a thin line of *Tc-fz2*-expressing cells marked the dorsal border between the extra-embryonic tissue and

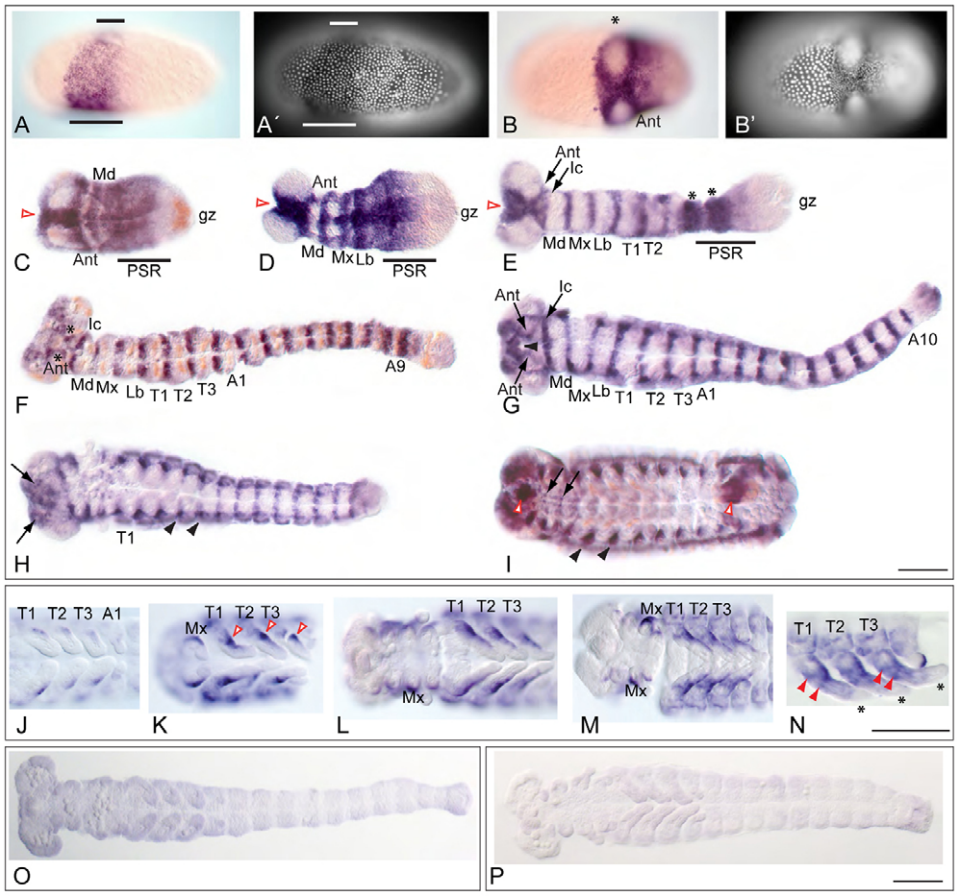

Fig. 2. *Tc-frizzled2* and *Tc-frizzled4* show a distinct expression pattern throughout embryonic development whereas *Tc-frizzled1* and *Tc-arrow* are ubiquitously expressed. *Tc-fz2* (A-I), *Tc-fz4* (J-N), *Tc-fz1* (O), *Tc-arrow* (P) in situ hybridisation or *Tc-fz2* and *Tc-wg* double in situ hybridisation (C,F,I) during *Tribolium* development. (**A**,**A′**) Blastoderm formation. *Tc-fz2* is expressed in the prospective head region (bars). A′ shows DAPI staining. (**B**,**B′**) In the germ anlage, *Tc-fz2* is expressed around the head lobes (asterisk). B′ shows DAPI staining. (**C-E**) Segmental stripes form, but in contrast to *Tc-wg* (red in C), the posterior growth zone (gz) stays free of *Tc-fz2* expression (blue) at all stages. *Tc-fz2* covers the presegmental region (PSR, bar), fading towards the posterior (C-E) (Schröder et al., 2008). Anteriorly, *Tc-fz2* is seen in the prospective clypeolabrum and stomodeum (open arrowheads). The intercalary segment (Ic, E) appears as well as two broad stripes in the PSR (bar), possibly the future T3 and A1 segments (asterisks). (**F**) Within the segments, *Tc-fz2* (blue) is expressed at the segmental border posterior to *Tc-wg* (red). The labrum is free of *Tc-fz2* expression. Asterisks indicate antennal segments. (**G**) Segmental expression of *Tc-fz2* in the fully elongated embryo. Arrowhead indicates the stomodeum. (**H**) Germband retraction. Segmental *Tc-fz2* expression declines, *Tc-fz2* expression appears in the visceral mesoderm, around the tracheal openings (arrowheads in H,I) and in the brain (arrows). (**I**) Fully retracted germband. *Tc-fz2* expression (blue) in the foregut and the hindgut (open arrowheads), in the CNS (arrows) and laterally in the visceral mesoderm (black arrowheads). *Tc-fz2* is at no time expressed in the legs, in contrast to *Tc-wg* (red). (**J-N**) *Tc-fz4* expression in a proximo-dorsal position during appendage elongation (open red arrowheads in K). Late in embryogenesis (N) *Tc-fz4* expression extends and marks the putative border of the trochanter (red arrowheads in N). No *Tc-fz4* expression (black asterisks) is observed in the distal tip. (**O**,**P**) *Tc-fz1* (O) and *Tc-arrow* (P) are ubiquitously expressed (representative stages shown). All views ventral, except A,A′ (lateral) and C,D (dorsal). A1-A10, abdominal segments 1-10; Ant, antennae; gz, growth zone; Lb, labial segment; Ic, intercalary segment; Md, mandibular segment; Mx, maxillar segment; PSR, presegmental region; T1-T3, thoracic segments 1-3. Scale bars: 100 μm.

the embryonic anlage (see Fig. S1 in the supplementary material). By the onset of gastrulation, *Tc-fz2* was strongly expressed around the procephalic lobes but excluded from the posterior egg pole (Fig. 2B,B′). Once the embryo started to segment, *Tc-fz2* transcripts were strongly expressed in the prospective labrum and in the antennal and mandibular segments (Fig. 2C). Posterior to the mandibular stripe and anterior to the posterior growth zone, a broad *Tc-fz2* expression domain that faded out towards the posterior covered the presegmental region (PSR). This central *Tc-fz2* domain did not overlap with *Tc-wingless* (*Tc-wg*) expression at the posterior end of the embryo (Fig. 2C). During AE, the emerging stripe pattern became evident (Fig. 2C-E). *Tc-fz2* expression persisted in one (Fig. 2C,D), and later two, broad stripes (Fig. 2E,F) in the PSR until the embryo was fully elongated (Fig. 2F,G). The segmental *Tc-fz2* stripes were out of register with the *Tc-wg* stripes (Fig. 2F). In the fully extended germband, *Tc-fz2* was expressed in the posterior part of each body segment, mapped by the relative position of *Tc-wg* (Fig. 2F). In the head, *Tc-fz2* expression was detected in the clypeolabral region, a region surrounding the stomodeum, and in the antennal and intercalary segments (Fig. 2G). By the time of germband shortening, the segmental pattern of *Tc-fz2* expression declined in the epidermis and increased in the visceral mesoderm and the gut anlagen (Fig. 2H,I). In the hindgut, *Tc-wg* was co-expressed with *Tc-fz2*, indicating a possible interaction (Fig. 2I). No *Tc-fz2* expression was observed in the larval legs, the growth zone proper or the most posterior cells (Fig. 2C-E,I).

Tc-fz4 was expressed in a dorso-proximal position in elongating legs in the coxa-trochanter region (Fig. 2J). As the legs continued to grow, this expression domain intensified, spread laterally and extended more distally without reaching the distal tip (Fig. 2K-M). When the legs had reached their full length, *Tc-fz4* expression was circumferential in the proximal leg region, encompassing most of the coxal region, the future trochanter and part of the tibiotarsus. Within this expression domain, *Tc-fz4* expression was modulated: transcripts were more abundant at the sites where the joints of the trochanter will form (Fig. 2N). The head appendages also expressed *Tc-fz4* in dorso-proximal positions (Fig. 2K-M). In all appendages, the distal tip lacked *Tc-fz4* expression throughout embryogenesis. By contrast, *Tc-fz1* and *Tc-arrow* were ubiquitously expressed throughout embryogenesis (Fig. 2O,P).

The combined function of *Tc-frizzled1* and *Tc-frizzled2* is essential for body axis elongation

To elucidate the functions of the different receptors, we depleted *Tc-fz1* and *Tc-fz2* by parental RNAi. Single *Tc-fz2* RNAi knockdown resulted in viable, wild-type progeny. However, double knockdown of *Tc-fz1* and *Tc-fz2* resulted in axis elongation defects ranging from mild to severe (Fig. 3). In weakly affected *Tc-fz1/2*^{RNAi} individuals, larval cuticles developed only one to two abdominal segments and a remnant of the hindgut. Abdominal segments three to eight and the posterior urogomphi were missing (Fig. 3B,C). The head and the thorax with their associated appendages developed normally. More strongly affected *Tc-fz1/2*^{RNAi} individuals displayed defects that affected the thorax and appendages. Nevertheless, the pregnathal region remained only weakly affected (Fig. 3C-E). The most strongly affected cuticles, which resulted from injections of a high dsRNA concentration, were of a spherical shape (Fig. 3D,E), with only a relic of head and thorax.

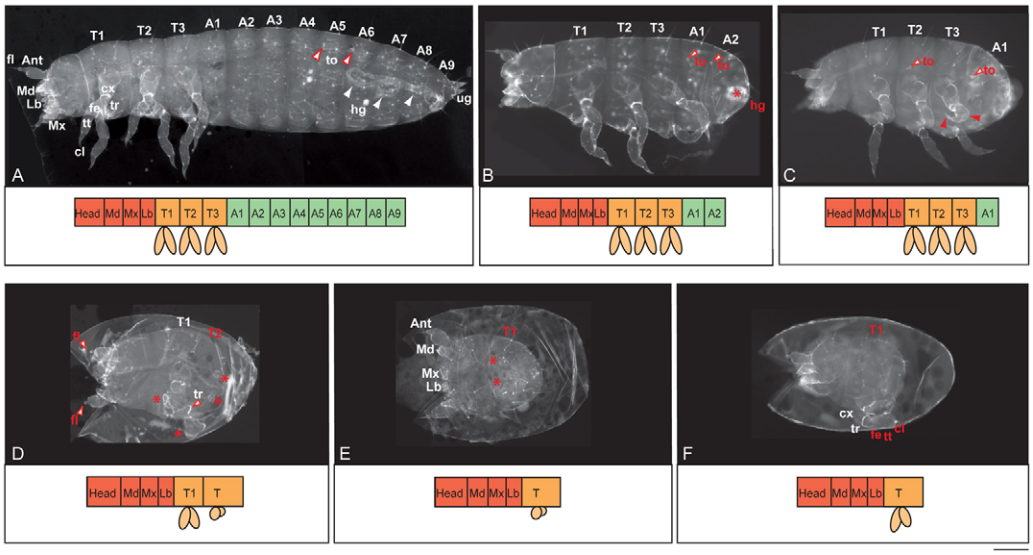

Fig. 3. *Tc-fz1/2*-dependent Wnt signalling is required for posterior growth and segmentation. Autofluorescence cuticle preparations with schematics of the corresponding phenotype below. (**A**) Wild-type-like cuticle. Head with head appendages, thoracic segments 1-3 (T1-3) each with one pair of legs, and eight abdominal segments (A1-8) with urogomphi at abdominal segment 9 (A9). Autofluorescence of the hindgut cuticle can be observed. (**B**) Weak *Tc-fz 1/2*^{RNAi} phenotype. Head and thorax with two abdominal segments marked by tracheal openings (arrowheads). A rudimentary hindgut (asterisk) is visible. (**C**) Intermediate *Tc-fz 1/2*^{RNAi} phenotype. Head, thorax with malformed legs and one abdominal segment. Tracheal openings (arrowheads) indicate the identity of T2 and A1. (**D**) Stronger *Tc-fz 1/2*^{RNAi} phenotype. Two thoracic segments with leg rudiments (asterisks). On the head only the antennal flagellae are missing. (**E**,**F**) Strongest *Tc-fz 1/2*^{RNAi} phenotypes. Head with malformed gnathal appendages and T1 (gnarled legs, asterisks). A1-A10, abdominal segments 1-10; Ant, antennae; cl, pretarsal claw; cx, coxa; fe, femur; fl, flagella; hg, hindgut; Lb, labial segment; Md, mandibular segment; Mx, maxillar segment; to, tracheal opening; T1-T3, thoracic segments 1-3; tr, trochanter; tt, tibiotarsus; ug, urogomphi. Red asterisks indicate affected cuticle structures. Scale bar: 100 μm.

Pair-rule gene expression is not completely abolished in *Tc-fz1/Tc-fz2*^{RNAi} embryos

To understand how the *Tc-fz1/Tc-fz2*^{RNAi} phenotype manifests during embryogenesis, we analysed the expression of marker genes prior to cuticle formation (Fig. 4). The primary pair-rule genes *even-skipped* and *odd-skipped* (Choe et al., 2006) are expressed in similar patterns in the posterior growth zone and presegmental region as well as segmental stripes in young wild-type embryos (Fig. 4A,F) (Brown et al., 1997; Choe et al., 2006; Patel et al., 1994).

The phenotypic series of the *Tc-fz1/2*^{RNAi} knockdown showed an increasing reduction of the growth zone tissue (Fig. 4B-E,G-J). Expression of *Tc*-Eve protein was ultimately reduced to a few cells at the posterior end, but was not completely abolished (Fig. 4E) as has been described for *Tc-torso*^{RNAi} embryos (Schoppmeier and Schröder, 2005) and *Tc-arrow*^{RNAi} embryos (Bolognesi et al., 2009). Expression of *odd-skipped* was reduced to one subterminal stripe (Fig. 4G,H) or was dramatically reduced in intensity but not completely eliminated (Fig. 4J). The segmental marker Engrailed (Fig. 4K-O) was expressed normally in the remaining head and thoracic segments of older embryos (Fig. 4L-O). The expression of *Tc-wingless* at the segmental borders of *Tc-fz1/2*^{RNAi} embryos was weak or absent, but segmental *Tc-wg* spots indicated the integrity of the remaining individual segments in older embryos (see Fig. S2 in the supplementary material). This finding has also been observed in *Tc-arrow*^{RNAi} embryos (Bolognesi et al., 2009).

In wild-type embryos (Fig. 4P), *Tc-wnt5* was prominently expressed in the posterior growth zone, in segmental stripes during germband elongation and at the tips of appendages. In the head, the transcripts were detected in wedge-shaped domains in the head lobes and in the antennal segment (Fig. 4P). No expression of the ligand *Tc-wnt5* was seen in *Tc-fz1/2*^{RNAi} embryos, except for the head-specific domain (Fig. 4Q,R).

Residual expression of the Wnt ligand *Tc-wnt8* in *Tc-fz1/2*^{RNAi} embryos displaying a strong phenotype (see Fig. S2A-C in the supplementary material) confirmed the presence of the posterior-most cells of the growth zone (see Fig. S2B,C in the supplementary material). In wild-type embryos (see Fig. S2A in the supplementary

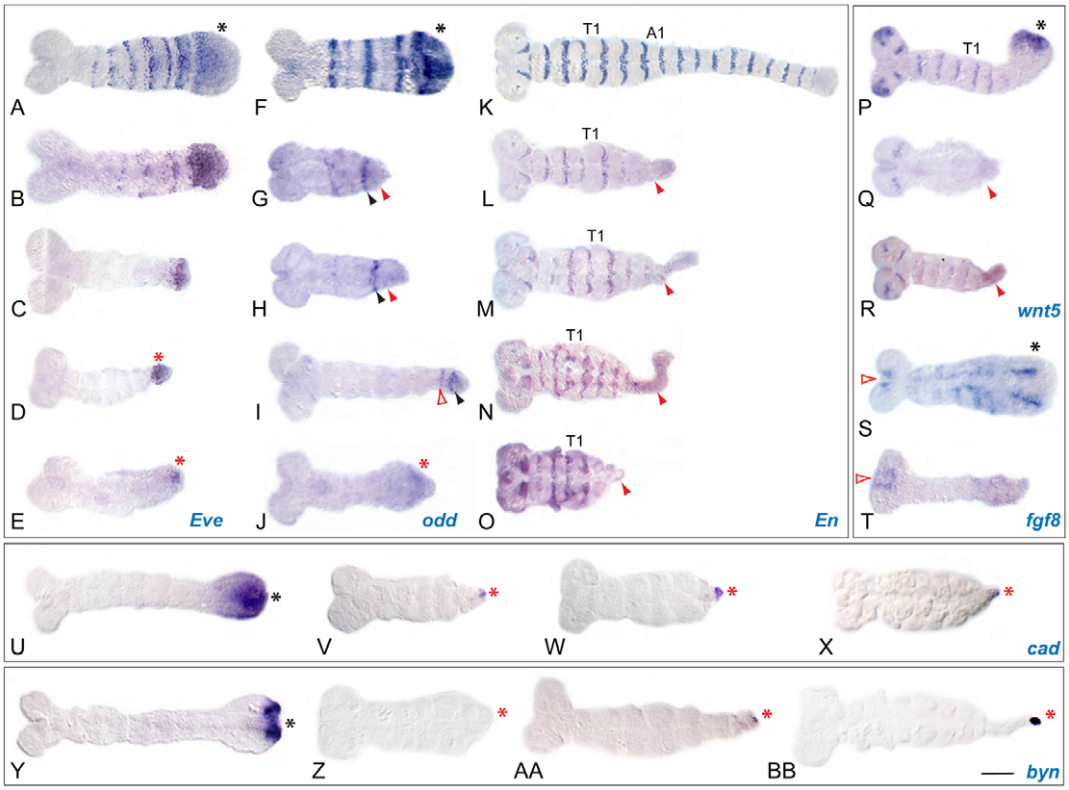

Fig. 4. The growth zone collapses in *Tc-fz1/2*^{RNAi} embryos. *Tc-fz1/2*^{RNAi} embryos of increasing phenotypic strength analysed for the expression of marker genes. (**A-J**) Pair-rule gene product Eve (A-E) and *odd-skipped* (*odd*; F-J) expression in wild-type (A, F) and *Tc-fz1/2*^{RNAi} (B-E,G-J) embryos. Even in the strongest phenotypes (C-E), a spot of Eve-positive cells is seen at the posterior, or a subterminal stripe of *odd* expression develops (red arrowhead in G,H; red asterisk in D,E,J). Both genes show only partial (weak phenotype in B) or no secondary pair-rule pattern. Pair-rule expression is initiated but not transformed into a segmental pattern anterior to the presegmental region (PSR; red asterisk), except for a weak stripe seen in B or I (open arrowhead). (**K-O**) Expression of the segment polarity gene product Engrailed (En) in wild-type (K) and *Tc-fz1/2*^{RNAi} (L-O) embryos. Integrity of segmental borders seems normal anterior to the growth zone rudiment (red arrowhead). Red arrowheads indicate collapsed growth zone. (**P-R**) Expression of the Wnt ligand *Tc-wnt5* in wild-type (P) and *Tc-fz1/2*^{RNAi} (Q,R) embryos. Stripes in the abdomen and expression domains in the posterior growth zone are gone (red arrowhead) but head spots and antennal stripes are not affected in the *Tc-fz1/2*^{RNAi} embryos. (**S**,**T**) Fgf ligand expression in wild-type (S) and *Tc-fz1/2*^{RNAi} (T) embryos. *Tc-fgf8* expression at the rims of the future mesoderm and within the segmented region is abolished but labral-specific domain (arrowhead) is unaffected in *Tc-fz1/2*^{RNAi} (T) embryos. (**U**) *Tc-caudal* expression at a posterior position in a wild-type embryo. (**V-X**) *Tc-caudal* expression marks posterior cells in *fz1/2*^{RNAi} embryos. (**Y**) *Tc-brachyenteron* (*byn*) marks the anlagen of the hindgut in the wild-type embryo. (**Z-BB**) *Tc-byn* expression is lost in strong *fz1/2*^{RNAi} embryos (Z) but retained in weaker *fz1/2*^{RNAi} embryos (AA,BB). A1, abdominal segment 1; T1, thoracic segment 1. Black asterisks indicate growth zone; red arrowheads indicate collapsed growth zone; red asterisks indicate affected structures. Scale bar: 100 μm.

material), *Tc-wnt8* expression is confined to a tiny horseshoe-shaped domain at the very posterior during a short time window extending from early blastoderm to the young embryo with few segments (Bolognesi et al., 2008a).

To test the connection of the Wnt pathway to other signalling pathways possibly involved in setting up segmentation and maintaining the growth zone in *Tribolium*, we evaluated the expression of *Tc-fgf8* in *Tc-fz1/2*-depleted embryos. In vertebrates, Fgf signalling is involved in somitogenesis of the embryo in a graded fashion (Delfini et al., 2005), and in *Drosophila* it influences the establishment of the germ layers, mesoderm development and cell migration (Klingseisen et al., 2009; McMahon et al., 2010). Although the embryonic FGF signalling sites in *Tribolium* have been characterised, the functional requirement for individual members of the FGF pathway remains to be shown (Beermann and Schröder, 2008). In young wild-type germ anlage *Tc-fgf8* is expressed in two small stripes bordering the prospective mesoderm in the growth zone. As the segments formed, transcripts were detected in small segmental blocks on both sides of the midline, potentially the segmental mesoderm, and anteriorly between the head lobes (Fig. 4S). In *Tc-fz1/2*-depleted embryos, *Tc-fgf8* expression was completely lost in the posterior region but persisted between the head lobes (Fig. 4T). Thus, posterior and segmental *Tc-fgf8* expression depends on *Tc-fz1/2*-mediated Wnt signalling. This finding provides a connection between the two signalling pathways, placing Wnt signalling upstream of Fgf signalling in segmentation. The existence of posterior cells in *Tc-fz1/2*^{RNAi} embryos during AE was demonstrated by the expression of the posterior marker gene *caudal* (Fig. 4V-X), whereas expression of the hindgut marker gene *brachyenteron* (*byn*) was seen only in less strongly affected *Tc-fz1/2*^{RNAi} embryos (Fig. 4AA,BB).

The Wnt co-receptor Tc-Arrow is involved in axis elongation, leg formation and segmentation

Knockdown of the Wnt co-receptor *Tc-arrow* by RNA interference resulted in a spectrum of leg phenotypes ranging from mild to severe (Fig. 5). In addition, embryos with reduced function of *Tc-arrow* developed consecutively fewer abdominal segments (Fig. 5A-H). Embryos with the mildest phenotype developed abdominal segments A1-5 with flattened urogomphi (Fig. 5A, arrowhead) and exhibited twisted legs. Embryos with a slightly stronger phenotype (Fig. 5B) had only four abdominal segments, and the leg segments distal to the coxa were severely shortened, twisted and fused (stars in Fig. 5B). In intermediate and strong *Tc-arrow*^{RNAi} phenotypes, the number of abdominal segments and the distal part of the legs were severely reduced or even absent. In the legs, only the proximal coxa (Fig. 5C,D) remained intact (Fig. 5E). The strongest phenotypes were characterised by a complete loss of segmentation, appendages and other cuticular markers (Fig. 5F-H) (Bolognesi et al., 2009).

Tc-Frizzled1 transmits Wnt signalling during appendage differentiation

RNAi knockdown of *Tc-Fz1* function interfered with the formation of the distal leg (Fig. 6A-E). In wild-type insects, the larval leg is stereotypically organised (Beermann et al., 2004) such that the coxa belongs to the body wall proper (Cohen et al., 1993) and is followed distally by the trochanter, the tibiotarsus and the pretarsal claw (Fig. 6A). In weakly affected *Tc-fz1*^{RNAi} larvae, the leg segments distal to the coxa appeared fused and twisted, giving them a bubbly appearance (Fig. 6D,E), whereas in stronger phenotypes, the segments distal to the coxa were fused into a club-like structure of uncertain composition (Fig. 6C). The most distal structures of the appendages, the pretarsal claw and setae of the antennae, were missing entirely (Fig. 6B,C-E). The coxa stayed

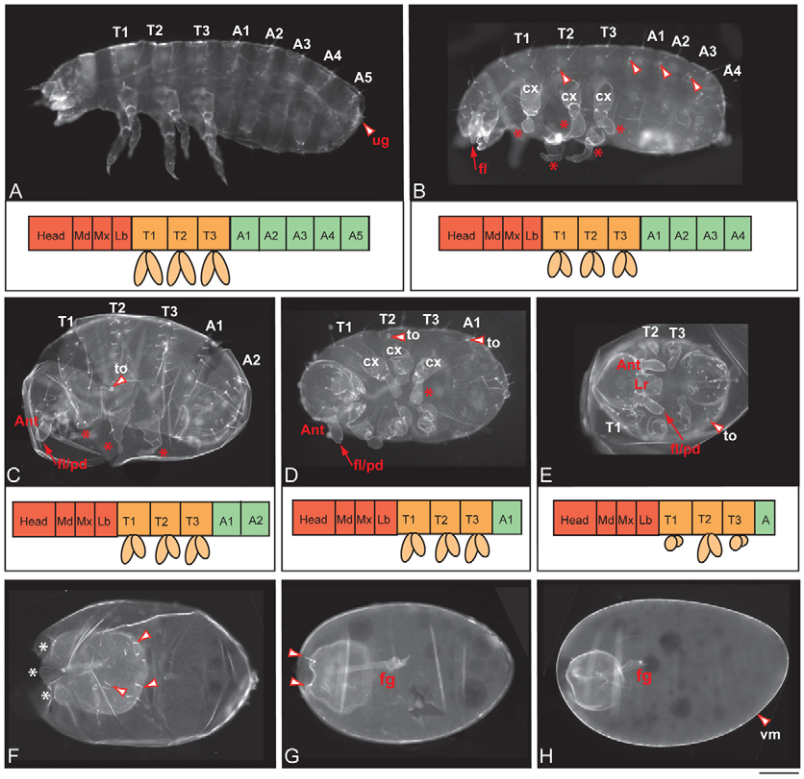

Fig. 5. Wnt co-receptor Arrow processes Wnt signals in axial growth, segmentation and leg formation. (**A**,**B**) Weak *Tc-arrow*^{RNAi} phenotype. Few abdominal segments missing, leg defects in B. Arrowheads in B indicate tracheal openings. (**C-E**) Intermediate *Tc-arrow*^{RNAi} phenotype. Few segments are developed, legs show abnormalities. (**F-H**) Strong *Tc-arrow*^{RNAi} phenotype. Cuticle spheres without signs of segmentation, with incomplete anterior head structures (white asterisks in F) and gut-like structure (fg) visible. A-C show a lateral view, D-F a ventral view. In A-E, schematics of the corresponding phenotypes are shown below. Red asterisks indicate affected cuticle structures. Open arrowheads in F,G indicate bristles. Ant, antennae; cx, coxa; fg, foregut; fl, flagella; Lr, labrum; pd, pedicellus; T1-T3, thoracic segments 1-3; to, tracheal opening; ug, urogomphi; vm, vitelline membrane; A1-A5 abdominal segments 1-5. Scale bar: 100 μm.

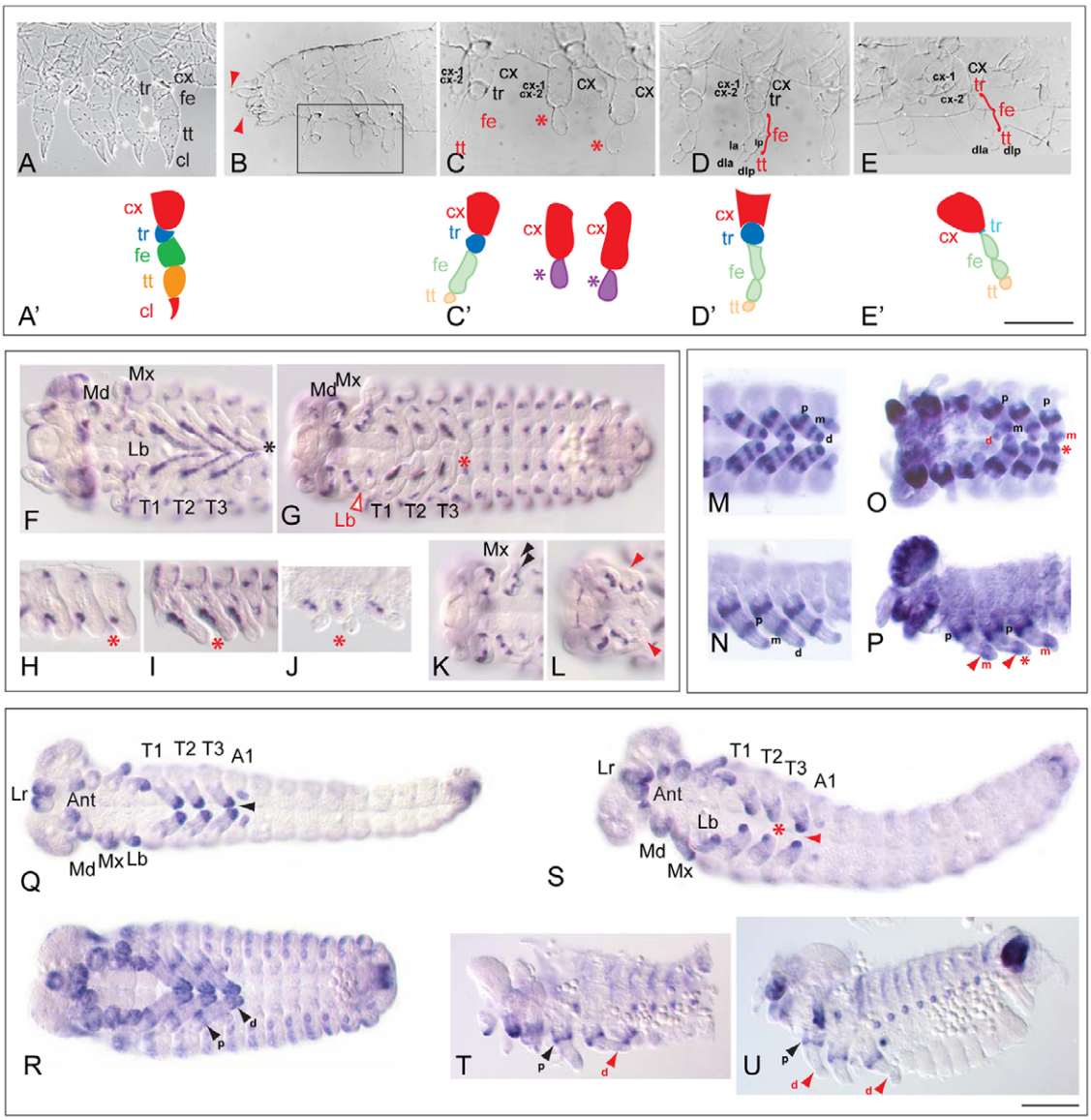

Fig. 6. *Tc-fz1* has an exclusive function in appendage differentiation. (**A**,**A'**) Wild-type larval leg showing coxa (cx), trochanter (tr), femur (fe), tibiotarsus (tt) and pretarsal claw (cl). Schematic of leg parts is shown in A'. (**B-C'**) *Tc-fz1*^{RNAi} larva. Legs have defects of the proximal-distal axis. (B) *Tc-fz1*^{RNAi} larva, anterior half. Antennae lack flagellae (red arrowheads). Boxed area in B is enlarged in C and illustrates a severe leg phenotype. Schematic is shown in C'. The coxa are unaffected according to coxa specific bristles cx-1 and cx-2 but femur and tibiotarsus are fused and twisted. There is no distinct identity of leg segments (asterisks and purple colour in C'), no pretarsal claw is present and the trochanter is fused to the coxa. (**D-E'**) Weaker *Tc-fz1*^{RNAi} phenotypes. Schematics of leg phenotypes are shown in C' and D'. (D,D') *Tc-fz1*^{RNAi} larva showing 'non-pareille' phenotype (Grossmann et al., 2009). Ectopic constriction in the femur, no pretarsal claw according to tibiotarsal bristle markers dla and dlp. Femur bristle markers la and lp are shown. (E,E') *Tc-fz1*^{RNAi} larva showing a stronger phenotype as in D. Trochanter is not clearly recognisable (blue in E'; 'pearls on a chain' phenotype) (Grossmann et al., 2009). (**F**) *Tc-wg* expression in wild type in all appendages, reaching in a ventral stripe to the tip of each leg (asterisk). (**G**) *Tc-wg* expression in a *Tc-fz1*^{RNAi} embryo is restricted to the coxa (red asterisk), appendages are distally fused and twisted (red asterisk). There is normal *Tc-wg* expression in the segments. (**H-J**) Consecutively older *Tc-fz1*^{RNAi} legs. *Tc-wg* expression remains proximal, restricted to coxa and never extends into the tips (asterisks). In J, the distal part of the legs shows the most severe defect (asterisks). (**K**) *Tc-wg* expression in wild-type head appendages. Maxillar lobes are present (arrowheads). (**L**) *Tc-wg* expression in *Tc-fz1*^{RNAi} head appendages. Maxillar palp is missing (red arrowhead). (**M**,**N**) In wild-type legs (ventral and lateral view) *Tc-Lim* is expressed in three domains: the proximal ring (p, coxa), the median ring (m, femur/tibia) and the distal domain (d). (**O**,**P**) *Tc-Lim* expression in *Tc-fz1*^{RNAi} legs, ventral and lateral view. Distal domain is missing or only partly present (red asterisks), the median ring (m) broadens (arrowheads). (**Q**,**R**) *Tc-dachsous* expression in wild-type appendages. In younger embryos, *dachsous* is expressed in a prominent distal domain in all appendages (Q), and later additionally in a proximal ring in the coxa (arrowheads in R). (**S-U**) *Tc-dachsous* expression in *Tc-fz1*^{RNAi} embryos. Distal expression in the legs is incomplete or missing, only proximal expression remains. (S) *Tc-fz1*^{RNAi} embryo with leg defects. The distal expression of *Tc-dachsous* is reduced (asterisk, arrowhead). (T,U) Older *Tc-fz1*^{RNAi} legs. Only the proximal expression of *Tc-dachsous* together with a very faint distal domain (arrowheads). Leg segment bristle markers: cx-1, coxa-1; cx-2, coxa-2. A1, abdominal segment 1; Ant, antennae; cl, pretarsal claw; cx, coxa; d, distal ring; dla, distal dorsal anterior; dlp, distal dorsal posterior; fe, femur; la, dorsal anterior; Lb, labial segment; lp, dorsal posterior; Lr, labrum; m, median ring; Md, mandibular segment; Mx, maxillar segment; p, posterior ring; T1-T3, thoracic segments 1-3; tr, trochanter; tt, tibiotarsus. Red asterisks indicate affected structures. Scale bar: 100 μm.

intact, as shown by the presence of the coxa-specific bristles cx-1 and cx-2 (Grossmann et al., 2009). Thus, *Tc-fz1*-dependent Wnt signalling is crucial for appendage elongation, as was previously reported for *wingless* in *Drosophila* (Kubota et al., 2003) and *Tribolium* (Grossmann et al., 2009).

To gain insight into the mechanistic cause of the leg phenotype, we analysed the embryonic *Tc-fz1*^{RNAi} phenotype using marker genes for the ventral (*Tc-wingless*; Fig. 6F-L) and the distal leg (*Tc-LIM1* and *Tc-dachsous*; Fig. 6M-U). In wild-type larvae, *Tc-wingless* was expressed in a ventral stripe in elongating legs and gnathal appendages (Fig. 6F,K). In *Tc-fz1*^{RNAi} embryos, *Tc-wg* expression in the distal parts of the appendages was abolished except for a ventral stripe in the coxa (Fig. 6G-J,L). Abdominal segmentation in *Tc-fz1*^{RNAi} embryos was normal (Fig. 6G).

The LIM homeobox gene *Tc-Lim1* showed three distinct expression domains. The most proximal ring of expression (p in Fig. 6M,N) corresponds to the coxa, the middle ring (m in Fig. 6M,N) to the femur and the most distal ring (d in Fig. 6M,N) to the distal tibiotarsus and the pretarsal claw (Pueyo et al., 2000; Tsuji et al., 2000). *Tc-Lim1* expression domains serve as markers for proximal, medial and distal positions in the embryonic leg anlage. *Tc-dachsous* marks the distal leg during elongation (Fig. 6Q) and is expressed in the coxa at older stages (Fig. 6R).

In *Tc-fz1*^{RNAi} embryos, both marker genes document the absence of the anlagen for the tibiotarsus and the pretarsal claw. In weaker leg phenotypes, the proximal and medial rings of *Tc-Lim1* expression were still present (Fig. 6O); however, only the most proximal ring remained intact in embryos displaying a stronger leg phenotype (Fig. 6P). Here, the distal ring was absent, whereas the middle expression domain was broadened, resulting in a fused and augmented femur (Fig. 6P). In all cases, the distal ends of the remaining legs were bent (Fig. 6O,P,S-U) and malformed.

In *Tc-fz1*^{RNAi} legs, the distal expression domain of *Tc-dachsous* was strongly reduced (Fig. 6S) or absent (Fig. 6T,U), consistent with the *Tc-fz1*^{RNAi} cuticle leg phenotypes (Fig. 6B-E). In summary, only the coxa, i.e. the proximal part of the leg, was intact in *Tc-fz1*^{RNAi} embryos and thus confirms the function of *Tc-fz1* in distal leg formation.

Tc-frizzled1/4 double RNAi enhances the strength and the frequency of the *Tc-fz1* leg phenotype and affects hindgut development

RNAi knockdown of both *Tc-fz1* and *Tc-fz4* resulted in a stronger phenotype than those seen in the *Tc-fz1* single RNAi experiments. Here, in addition to weaker phenotypes that were indistinguishable from those induced by *Tc-fz1*-RNAi (Fig. 7A), more strongly affected legs presenting only the proximal coxa were observed (Fig. 7B). Moreover, *Tc-fz1/4*^{RNAi} larvae developed with a malformed hindgut (Fig. 7G). Interestingly, *Tc-fz1/4* double knockdown led to a higher percentage of affected embryos (see Table S1 in the supplementary material) than the respective single RNAi knockdowns. In the single *Tc-fz4* RNAi knockdown, no specific phenotypes above background levels were seen (see Table S1 in the supplementary material).

DISCUSSION

We have analysed the expression patterns and functions of the genes coding for the Wnt receptors (*frizzled 1*, *2* and *4*) and the Wnt co-receptor *Tc-arrow* during embryogenesis of the short germ beetle *Tribolium*. We reveal a redundant and combinatorial code of Wnt receptors and a co-receptor that regulates segmentation, axis elongation, leg formation and gut development in *Tribolium*.

Wnt receptors and co-receptors in the *Tribolium* genome

Whereas mammals possess ten unique Frizzled receptors, only four are present in the genomes of *Drosophila*, *Caenorhabditis elegans* and the cnidarian *Nematostella* (van Amerongen and Nusse, 2009). *Tribolium* has three frizzled orthologues, with no orthologue for *Drosophila fz3*. Thus, the number of *Tribolium* frizzled genes is not dramatically different from that of other insects or *Nematostella*, indicating that *frizzled1* and *2* as well as the structurally similar *frizzled 3* and *frizzled4* genes constituted a basic Wnt receptor set in the last common ancestor of *Nematostella* and insects.

The *Tribolium* genome contains two similar genes that code for LRP orthologues. We identified Tc008151 as the single Arrow/LRP5-6 Wnt co-receptor and performed the aforementioned experiments with this gene. The second LDL receptor, TC007146, represents the *Tribolium LRP4* orthologue – a putative Wnt antagonist (Fig. 1C). Prior to our analysis, the *Tribolium arrow* orthologue had been mistakenly assigned to the accession number Xm001814907 (Bolognesi et al., 2009), which actually represents the *LRP4* orthologue (Fig. 1). As our results on *Tc-arrow* function overlap with those of Bolognesi et al., we presume that their published results do indeed describe the function of the *Tribolium* Arrow orthologue. Interfering with LRP4 function in *Tribolium* results in a different phenotype than that shown for *Tc-arrow*^{RNAi} (R.P. and R.S., unpublished).

Wnt receptors and the co-receptor show specific and ubiquitous expression patterns

In *Tribolium*, *Tc-fz2* and *Tc-fz4* show distinct expression patterns, whereas *Tc-fz1* and *Tc-arrow* are ubiquitously expressed. Thus, *Tc-fz1*-mediated Wnt signalling could potentially occur throughout the entire embryo at all stages. Several tissues are marked by the expression of *Tc-fz2* or *Tc-fz4*, indicating specific Frizzled-dependent Wnt signalling sites. *fz2* expression sites are similar in *Tribolium* and *Drosophila* in late developmental stages (Bhanot et al., 1996). Exceptional for *Tribolium* is the strong expression in the head anlage observed at the blastoderm stage. However, no head defect was observed in *Tc-fz1/2*^{RNAi} embryos. This finding might be explained by a functional redundancy between Fz1, Fz2 and Arrow. We were able to rule out a combined involvement of Tc-fz1 or Tc-fz2 with Arrow in head development because the double RNAi experiments *Tc-fz1*/*arrow* and *Tc-fz2*/*arrow* did not result in head phenotypes (data not shown).

Functional analysis of the frizzled genes identifies the presegmental region as crucial for axial elongation

The *Tc-fz2* expression pattern and the *Tc-fz1/2* double RNAi phenotype identify the region between the posterior growth zone and the new segments as crucial for axial elongation (AE). This tissue develops in a similar position to the presomitic mesoderm (PSM) in vertebrates and is called the presegmental region (PSR) in *Tribolium* (Schröder et al., 2008). In both *Drosophila* and *Tribolium*, Fz1 and Fz2 function redundantly: in *Drosophila* during segmentation and in *Tribolium* within the PSR, the axis elongation phenotype was only seen when Tc-Fz1 and Tc-Fz2 were depleted simultaneously. As Wnt signalling drives segmentation from within the PSR, reception of the Wnt signal in this tissue by the Tc-Fz1 and Tc-Fz2 receptors is necessary for this process.

Our marker gene analysis showed that the posterior growth zone is not completely abolished in *Tc-fz1/2*^{RNAi} embryos, as was previously shown for *Tc-arrow*^{RNAi} embryos (Bolognesi et al., 2009). The markers Eve, *odd* and *wnt8* (Fig. 4, see Fig. S2 in the supplementary material) are still expressed in posterior cells of the growth zone. The persistent expression of the marker gene *caudal* (Fig. 4V-X) proves the identity of these cells as posterior cells. Because the complete wild-type expression pattern of *caudal* is not retained in *Tc-fz1/2*^{RNAi} embryos, the terminal-most tissues could still contribute to axis elongation. The absence of the hindgut marker *brachyenteron* (Fig. 4Z,AA) in strongly affected *Tc-fz1/2*^{RNAi} embryos is in accordance with the loss of the hindgut in *fz1/2*^{RNAi} larval cuticles (Fig. 3B-F). In less strongly affected *Tc-fz1/2*^{RNAi} embryos, *byn* expression is still detectable (Fig. 4AA,BB). Our results show that the transition of the pair-rule genes from the primary to the segmental phase (Choe et al., 2006; Patel et al., 1994) depends on Wnt signalling. As a consequence of this loss of Wnt signalling, AE does not occur. In contrast to *Tc-wnt8*, *Tc-wnt5* expression is completely abolished in strong *Tc-fz1/2*^{RNAi} embryos. This finding could be explained by an autoregulatory loop in the PSR involving Frizzled and Wnt5.

Tissue analogy between the PSM of vertebrates and the PSR of insects

In vertebrates, coordinated cell movements in the PSM under the control of FGF signalling are responsible for AE (Bénazéraf et al., 2010). Because signalling pathways are connected to other signalling pathways (van Amerongen and Nusse, 2009), we hypothesised that FGF signalling might be involved in AE in *Tribolium* as well. Indeed, the prominent wild-type FGF expression domain is missing in *Tc-fz1/2*^{RNAi} embryos (Fig. 4T), indicating that FGF signalling depends on Wnt signalling in *Tribolium* and might itself be crucially required for AE. It is striking that in both vertebrates and insects, a tissue immediately posterior to the last somites or segment formed – the PSM and the PSR, respectively – fulfils analogous functions in the axial elongation process.

Tc-fz1 single RNAi leads to specific defects in the distal leg

In *Drosophila* and *Tribolium*, *wingless* is required for segmentation as well as for distalisation and dorso-ventral patterning of the appendages (Cohen and Jürgens, 1989; Grossmann et al., 2009; Ober and Jockusch, 2006). For *Tribolium*, it was argued that the leg patterning function of *wingless* is only required during later embryonic stages (Grossmann et al., 2009).

We show that *Tc-fz1* function is required for both proximo-distal (PD) and dorso-ventral (DV) axis formation in the leg. Because both the PD and the DV leg phenotypes are the result of parental RNAi, we could not verify a distinct time-dependency for *Tc-fz1* function. Rather, our data support concentration-dependent regulation of the PD and DV axes during leg development. The *Tc-fz1*^{RNAi} leg phenotype strongly resembles the *wingless*^{RNAi} phenotypes described for *Tribolium* (Grossmann et al., 2009) and *Drosophila* (Diaz-Benjumea and Cohen, 1993; Diaz-Benjumea and Cohen, 1994). Based on bristle mapping, we propose that the best candidate ligand for Tc-Fz1 in appendage formation is Tc-Wnt1.

Remarkably, *Tc-fz1/2*^{RNAi} larvae lacking most of the abdominal segments develop normal legs (Fig. 3B). Here, the reduced *Tc-fz1* function seems to be partially compensated. This result is in contrast to *Tc-arrow*^{RNAi}, in which leg formation is severely affected in larvae with a mild AE defect (Fig. 5B). Why does the knockdown of *Tc-fz1* in the *Tc-fz1/2* double RNAi experiment only interfere mildly with leg formation? AE is apparently very sensitive to depletion of *Tc-fz1/2* function. The dose of dsRNA required for an AE phenotype hardly affects Tc-Fz1-dependent leg patterning at all. Presumably, in the double knockdown embryos, the concentration of *Tc-fz1* transcripts does not sink below a critical threshold. On the other hand, AE and leg patterning require similar amounts of the co-receptor Arrow. These results support a dosage dependency of Wnt receptors and co-receptors during embryogenesis.

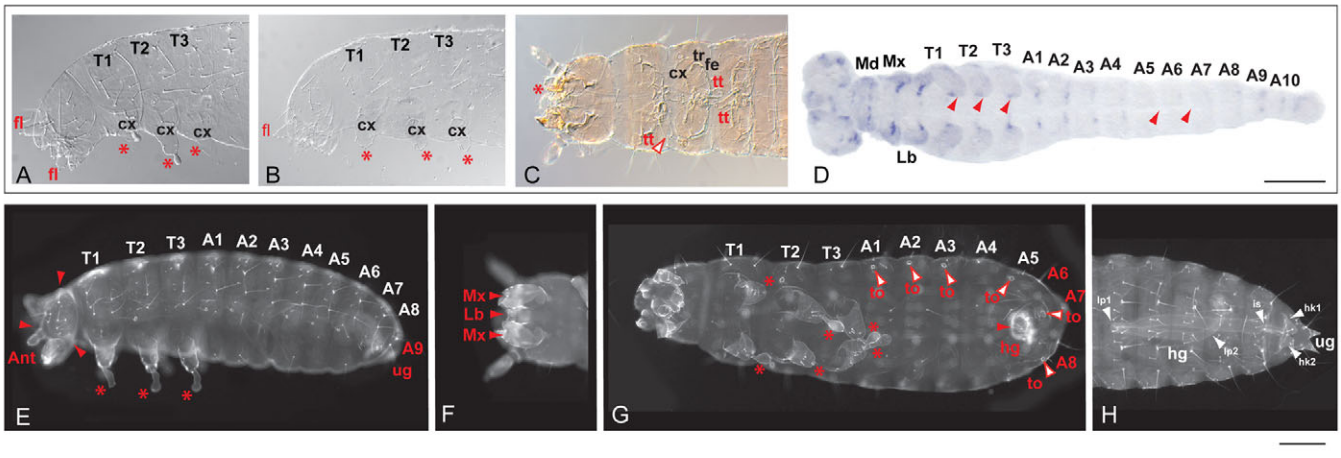

Fig. 7. *TcFz4* and the enhancement of the *TcFz1*^{RNAi} phenotype. (**A-C**) *Tc-fz1/4*^{RNAi} leads to loss of distal leg structures. In weaker phenotypes, segments of unclear identity adhere to the proximal leg (A); only the coxa is left in strong *Tc-fz1/4*^{RNAi} larvae (B). *Tc-fz1/4*^{RNAi} larvae can hatch but die as L2 larvae (C). (**D**) *Tc-wg* expression is noticeably reduced in the legs and the abdominal segments (arrowheads). (**E-G**) Additional defects of *Tc-fz1/4*^{RNAi} larvae. Slight head segmentation defects, missing urogomphi (E), maxillae and labium shortened (F). Hindgut is not elongated and divided (G). Subtle changes in the shape of the tracheal openings (open arrowheads, G). (**H**) Wild-type cuticularised hindgut (autofluorescence). Two loops (lp1,2), connected via the intersection (is) with two hooks (hk1, 2) to the outside. This division is absent in *Tc-fz1/4*^{RNAi} larvae. A1-A10, abdominal segments 1-10; cx, coxa; fe, femur; fl, flagella; hg, hindgut; Lb, labial segment; Mx, maxillar segment; T1-T3, thoracic segments 1-3; to, tracheal opening; tr, trochanter; tt, tibiotarsus; ug, urogomphi. Red asterisks mark affected cuticle structures. Scale bar: 100 μm.

Tc-fz1 functions in the distal leg and in combination with *Tc-fz4* in the proximal leg

In larvae with weak *Tc-fz1* RNAi phenotypes, lesions occur in the proximal leg, affecting the joints of the trochanter – sites of *Tc-fz4* expression (Fig. 2N) – and leading to a fusion of coxa and trochanter (Fig. 6C,C′). Tc-Fz4, therefore, supports Tc-Fz1 in transducing the Wnt signal in the proximal leg (Fig. 8B). This assumption is corroborated by the finding that *Tc-fz1/4* double RNAi enhances the frequency and the phenotype of this leg phenotype (see Table S1B in the supplementary material and Fig. 7G). However, Tc-Fz4 on its own is dispensable in the leg; Tc-Fz1 appears to be the crucial partner. At present, the precise function of Tc-Fz1/Fz4 in the dorso-proximal leg is speculative. The hypothesised leg differentiation centre at the coxa/trochanter boundary, postulated for *Tenebrio* (Huét and Lenoir-Rousseaux, 1976), is an intriguing possibility. Larvae with the strongest *Tc-fz1*^{RNAi} phenotype display loss of distal structures, including the pretarsal claw (Fig. 6C). Because *Tc-fz4* is not expressed distal to the tibiotarsal region, Tc-Fz1 seems to be the single primary Wnt transducer in the distal appendage (Fig. 8B). The ligand for this signal is probably distal Wnt1, based on the leg phenotype of *wg*^{RNAi} larvae (Grossmann et al., 2009). Depending on their conformation, Frizzled receptor proteins have been proposed to signal via different downstream signalling pathways and could thus serve as multifunctional signal transducers depending on, e.g. ligand availability (Carron et al., 2003). In this way, a variety of different biological outcomes can be controlled by a small number of Wnt receptors.

Redundant function of *Tc-fz1* and *Tc-fz4* in hindgut development

Double *Tc-fz1/4*^{RNAi} embryos reveal an additional function of the two receptors in hindgut formation. Although a normal hindgut develops in the respective single RNAi experiments, the elongation of the gut tubule is impaired in *Tc-fz1/4*^{RNAi} larvae; only remnants of the hindgut-specific cuticle develop (Fig. 7G). *Tc-fz1/4*^{RNAi} larvae survive to stage L2 (Fig. 7C) but subsequently die, probably due to a non-functional hindgut and stunted mouth appendages. A similar gut phenotype has been observed in *brachyenteron*^{RNAi} experiments (Berns et al., 2008) indicating that *Tc-byn* and *Tc-Fz4* might function within the same pathway. Indeed, *byn* has been shown to be a target of the Wnt signalling cascade in vertebrates (Arnold et al., 2000; Yamaguchi et al., 1999). Alternatively, elongation of the gut might be achieved via convergent extension under the combined control of *Tc-frizzled 1* and *Tc-frizzled 4*, pointing to the involvement of the planar cell polarity pathway.

Surprisingly, *wingless* expression in the segments is strongly reduced in *Tc-fz1/4*^{RNAi} embryos (Fig. 7D). The continued expression of *wingless* during segmentation therefore seems to depend on a feedback loop involving both Frizzled1 and Frizzled4. Because the abdominal segments form normally in *Tc-fz1/4*^{RNAi} embryos (Fig. 7E,G), the loss of *wingless* expression does not interfere with segmentation.

Arrow functions as the obligatory Wnt co-receptor

The requirement of Tc-Arrow for leg formation, AE and segmentation identifies this protein as an obligatory co-receptor in all these processes. We explain the spectrum of *Tc-arrow*^{RNAi} phenotypes, ranging from weak to strong (Fig. 5), by the declining amounts of ds-Tc-*arrow* RNA transferred by the injected mothers to their offspring during successive egglays. This ‘phenotypic series’ might point to a dosage dependency at the level of Wnt reception. In such a scenario, leg formation and AE would be most sensitive to the loss of Tc-Arrow function, whereas segmentation is more robust and only requires low concentrations of Arrow. This

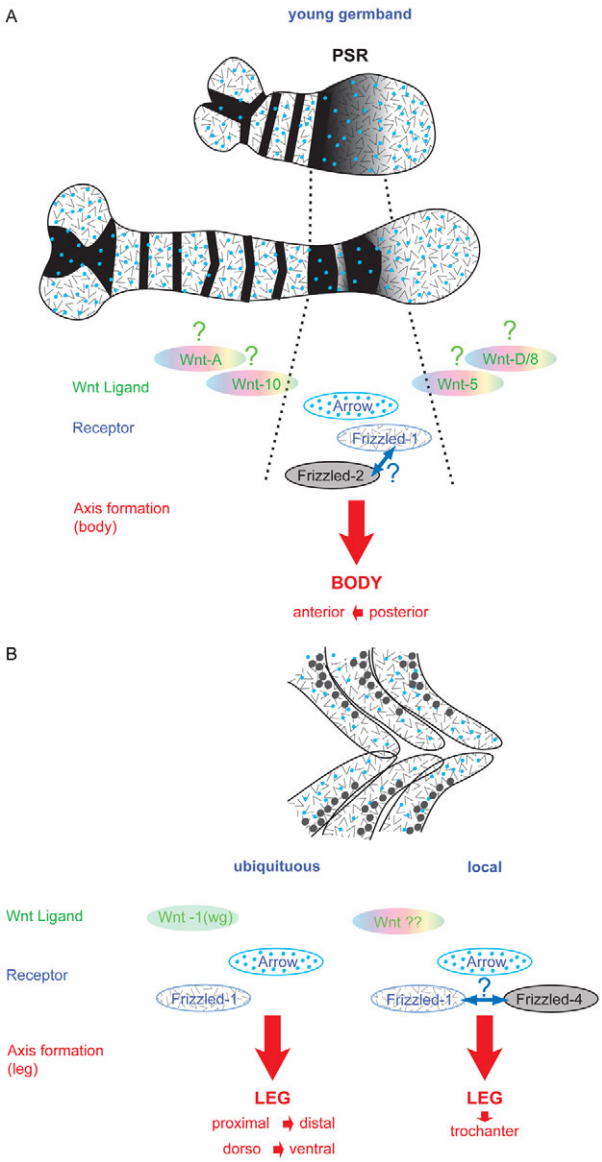

Fig. 8. The ‘combinatorial code’ model. (**A**) Summary of expression patterns and possible receptor/co-receptor interactions in the presegmental region (PSR) during anterior-posterior axis formation. *Tc-fz2* expression is shown in black in the segments and in the PSR. Within the PSR, *Tc-fz2* shows a graded expression fading out towards the posterior. *Tc-fz2* is always coexpressed with the ubiquitously expressed *Tc-fz1* and *Tc-arrow* (chevrons and blue dots, respectively). In these regions, it is possible that various dimeric forms (homo- or heterodimers) could form. In the young germ anlage, *Tc-wnt5* expression is close to the *Tc-fz2* expression domain (Fig. 4P). Later in embryogenesis, Tc-WntA and Tc-Wnt10 can serve as additional/alternate ligands for Tc-Fz1 and Tc-Fz2 in the PSR. (**B**) Summary of expression patterns and possible receptor/co-receptor interactions in the leg during proximo-distal axis formation. Ubiquitously expressed *Tc-Fz1* and *Tc-Arrow* are joined in a dorso-proximal position by *Tc-Fz4* (black dots). Here, Tc-Fz4 supports Wnt signalling by an as yet unknown Wnt ligand. In more distal and ventral positions, Tc-Fz1 and Tc-Arrow exclusively transduce Wnt1 signalling.

hypothesis is supported by the higher percentage of weaker *Tc-arrow*^{RNAi} phenotypes in RNAi experiments with concentrations of 10 ng/μl compared with the injection series with 50 ng/μl or higher (see Table S1B6 in the supplementary material).

Interestingly, specific defects in the larva were obtained only when the ubiquitously expressed genes *Tc-fz1* and *Tc-arrow* were knocked down, i.e., not when the genes showing distinct expression patterns (*Tc-fz2* or *Tc-fz4*) were depleted. The acquisition of new expression domains during evolution can promote the formation of embryonic parts with novel structural and functional aspects. We speculate that such a scenario could apply to the *Tc-fz2* and *Tc-fz4* genes.

Possible Wnt ligand-receptor combinations

Previous studies analysed the function of *wingless* (Grossmann et al., 2009) and *wnt8* (Bolognesi et al., 2008b). As no functional data for other Wnt molecules are available, the identities of the Wnt ligands that activate the Frizzled receptors during these embryological processes remain unclear. Our speculations are based on the expression patterns of the different Wnt ligands (Bolognesi et al., 2008a) (see Fig. S5 in the supplementary material) and are summarised in Fig. 8.

Further diversification of signalling outcomes could be achieved by the formation of homo- or heterodimers of Frizzled receptors via their cysteine-rich-domains. Such dimerisation events have been shown to occur in vitro for various vertebrate Frizzled proteins and other G-protein-coupled receptors (Angers et al., 2002; Carron et al., 2003; Dann et al., 2001; Milligan, 2004; Schulte and Bryja, 2007; Stiegler et al., 2009). Whether the Frizzled proteins function as independent monomers, homodimers or heterodimers in *Tribolium* is unknown. Fz1 and Fz2 in the PSR and Fz1 and Fz4 in the proximal leg could potentially form various receptor combinations (displayed in Fig. 8).

In conclusion, we have shown that a variety of tissue-specific outcomes are guided by a combinatorial code of three Wnt receptors and one Wnt co-receptor in *Tribolium*. We have identified the presegmental region in the *Tribolium* embryo as the necessary tissue for axis elongation at the Wnt receptor level and uncovered a network of signalling pathways within the PSR that controls this process. Our findings provide parallels to the involvement of FGF and Wnt signalling in vertebrate development (Dequéant and Pourquié, 2008). Both the FGF and Wnt signalling pathways are involved in axial patterning and serve as crucial regulators of animal embryogenesis. Future work will aim to identify the correct receptor-ligand combinations in the presegmental region and the appendages to disclose the complexity of the Wnt signalling pathway in short germ insects.

Acknowledgements

We gratefully acknowledge Rolf Reuter for continuous and generous support, T. Mader and A. Hlawa for excellent technical assistance, P. Spahn for reading drafts of the manuscript and the German Research Council (DFG) for its long-standing and continuous funding. The Even-skipped (2B8) and the Engrailed (4D9) monoclonal antibodies developed by N. Patel were obtained from the Developmental Studies Hybridoma Bank developed under the auspices of the NICHD and maintained by The University of Iowa, Department of Biological Sciences, Iowa City, IA 52242.

Competing interests statement

The authors declare no competing financial interests.

Supplementary material

Supplementary material for this article is available at
http://dev.biologists.org/lookup/suppl/doi:10.1242/dev.063644/-/DC1

References

Angers, S., Salahpour, A. and Bouvier, M. (2002). Dimerization: an emerging concept for G protein-coupled receptor ontogeny and function. *Annu. Rev. Pharmacol. Toxicol.* **42**, 409-435.

Arnold, S. J., Stappert, J., Bauer, A., Kispert, A., Herrmann, B. G. and Kemler, R. (2000). Brachyury is a target gene of the Wnt/beta-catenin signaling pathway. *Mech. Dev.* **91**, 249-258.

Aulehla, A., Wiegraebe, W., Baubet, V., Wahl, M. B., Deng, C., Taketo, M., Lewandoski, M. and Pourquié, O. (2008). A beta-catenin gradient links the clock and wavefront systems in mouse embryo segmentation. *Nat. Cell Biol.* **10**, 186-193.

Beermann, A. and Schröder, R. (2008). Sites of Fgf signalling and perception during embryogenesis of the beetle *Tribolium castaneum*. *Dev. Genes Evol.* **218**, 153-167.

Beermann, A., Aranda, M. and Schröder, R. (2004). The Sp8 zinc-finger transcription factor is involved in allometric growth of the limbs in the beetle *Tribolium castaneum*. *Development* **131**, 733-742.

Bénazéraf, B., Francois, P., Baker, R. E., Denans, N., Little, C. D. and Pourquié, O. (2010). A random cell motility gradient downstream of FGF controls elongation of an amniote embryo. *Nature* **466**, 248-252.

Berns, N., Kusch, T., Schröder, R. and Reuter, R. (2008). Expression, function and regulation of *Brachyenteron* in the short germ insect *Tribolium castaneum*. *Dev. Genes Evol.* **218**, 169-179.

Bhanot, P., Brink, M., Samos, C. H., Hsieh, J. C., Wang, Y., Macke, J. P., Andrew, D., Nathans, J. and Nusse, R. (1996). A new member of the *frizzled* family from *Drosophila* functions as a Wingless receptor. *Nature* **382**, 225-230.

Bolognesi, R., Beermann, A., Farzana, L., Wittkopp, N., Lutz, R., Balavoine, G., Brown, S. J. and Schröder, R. (2008a). *Tribolium* Wnts: evidence for a larger repertoire in insects with overlapping expression patterns that suggest multiple redundant functions in embryogenesis. *Dev. Genes Evol.* **218**, 193-202.

Bolognesi, R., Farzana, L., Fischer, T. D. and Brown, S. J. (2008b). Multiple Wnt genes are required for segmentation in the short-germ embryo of *Tribolium castaneum*. *Curr. Biol.* **18**, 1624-1629.

Bolognesi, R., Fischer, T. D. and Brown, S. J. (2009). Loss of *Tc-arrow* and canonical Wnt signaling alters posterior morphology and pair-rule gene expression in the short-germ insect, *Tribolium castaneum*. *Dev. Genes Evol.* **219**, 369-375.

Brown, S. J., Parrish, J. K., Beeman, R. W. and Denell, R. E. (1997). Molecular characterization and embryonic expression of the *even-skipped* ortholog of *Tribolium castaneum*. *Mech. Dev.* **61**, 165-173.

Bucher, G., Scholten, J. and Klingler, M. (2002). Parental RNAi in *Tribolium* (Coleoptera). *Curr. Biol.* **12**, R85-R86.

Cadigan, K. M. and Nusse, R. (1997). Wnt signaling: a common theme in animal development. *Genes Dev.* **11**, 3286-3305.

Carron, C., Pascal, A., Djiane, A., Boucaut, J.-C., Shi, D.-L. and Umbhauer, M. (2003). Frizzled receptor dimerization is sufficient to activate the Wnt/beta-catenin pathway. *J. Cell Sci.* **116**, 2541-2550.

Chen, C. M. and Struhl, G. (1999). Wingless transduction by the Frizzled and Frizzled2 proteins of Drosophila. *Development* **126**, 5441-5452.

Choe, C. P., Miller, S. C. and Brown, S. J. (2006). A pair-rule gene circuit defines segments sequentially in the short-germ insect *Tribolium castaneum*. *Proc. Natl. Acad. Sci. USA* **103**, 6560-6564.

Cohen, B., Simcox, A. A. and Cohen, S. M. (1993). Allocation of the thoracic imaginal primordia in the *Drosophila* embryo. *Development* **117**, 597-608.

Cohen, S. M. and Jürgens, G. (1989). Proximal-distal pattern formation in *Drosophila*: cell autonomous requirement for *Distal-less* gene activity in limb development. *EMBO J.* **8**, 2045-2055.

Copf, T., Schröder, R. and Averof, M. (2004). Ancestral role of *caudal* genes in axis elongation and segmentation. *Proc. Natl. Acad. Sci. USA* **101**, 17711-17715.

Dann, C. E., Hsieh, J. C., Rattner, A., Sharma, D., Nathans, J. and Leahy, D. J. (2001). Insights into Wnt binding and signalling from the structures of two Frizzled cysteine-rich domains. *Nature* **412**, 86-90.

Delfini, M. C., Dubrulle, J., Malapert, P., Chal, J. and Pourquié, O. (2005). Control of the segmentation process by graded MAPK/ERK activation in the chick embryo. *Proc. Natl. Acad. Sci. USA* **102**, 11343-11348.

Dequéant, M.-L. and Pourquié, O. (2008). Segmental patterning of the vertebrate embryonic axis. *Nat. Rev. Genet.* **9**, 370-382.

Diaz-Benjumea, F. J. and Cohen, S. M. (1993). Interaction between dorsal and ventral cells in the imaginal disc directs wing development in *Drosophila*. *Cell* **75**, 741-752.

Diaz-Benjumea, F. J. and Cohen, S. M. (1994). *wingless* acts through the *shaggy/zeste-white 3* kinase to direct dorsal-ventral axis formation in the *Drosophila* leg. *Development* **120**, 1661-1670.

Grossmann, D., Scholten, J. and Prpic, N. M. (2009). Separable functions of *wingless* in distal and ventral patterning of the *Tribolium* leg. *Dev. Genes Evol.* **219**, 469-479.

Habas, R. and Dawid, I. B. (2005). Dishevelled and Wnt signaling: is the nucleus the final frontier? *J. Biol.* **4**, 2.

Hsieh, J. C., Rattner, A., Smallwood, P. M. and Nathans, J. (1999). Biochemical characterization of Wnt-frizzled interactions using a soluble, biologically active vertebrate Wnt protein. *Proc. Natl. Acad. Sci. USA* **96**, 3546-3551.
Huét, C. and Lenoir-Rousseaux, J. J. (1976). Étude de la mise en place de la patte imaginale de *Tenebrio molitor*. *J. Embryol. Exp. Morphol.* **35**, 303-321.
Huson, D. H., Richter, D. C., Rausch, C., Dezulian, T., Franz, M. and Rupp, R. (2007). Dendroscope: an interactive viewer for large phylogenetic trees. *BMC Bioinformatics* **8**, 460.
Janssen, R., Le Gouar, M., Pechmann, M., Poulin, F., Bolognesi, R., Schwager, E. E., Hopfen, C., Colbourne, J. K., Budd, G. E., Brown, S. J. et al. (2010). Conservation, loss, and redeployment of Wnt ligands in protostomes: implications for understanding the evolution of segment formation. *BMC Evol. Biol.* **10**, 374.
Kennerdell, J. R. and Carthew, R. W. (1998). Use of dsRNA-mediated genetic interference to demonstrate that *frizzled* and *frizzled 2* act in the *wingless* pathway. *Cell* **95**, 1017-1026.
Kim, H. S., Murphy, T., Xia, J., Caragea, D., Park, Y., Beeman, R. W., Lorenzen, M. D., Butcher, S., Manak, J. R. and Brown, S. J. (2010). BeetleBase in 2010, revisions to provide comprehensive genomic information for *Tribolium castaneum*. *Nucleic Acids Res.* **38**, D437-D442.
Klingseisen, A., Clark, I. B., Gryzik, T. and Muller, H. A. (2009). Differential and overlapping functions of two closely related *Drosophila* FGF8-like growth factors in mesoderm development. *Development* **136**, 2393-2402.
Kubota, K., Goto, S. and Hayashi, S. (2003). The role of Wg signaling in the patterning of embryonic leg primordium in *Drosophila*. *Dev. Biol.* **257**, 117-126.
Logan, C. Y. and Nusse, R. (2004). The Wnt signaling pathway in development and disease. *Annu. Rev. Cell Dev. Biol.* **20**, 781-810.
Martin, B. L. and Kimelman, D. (2009). Wnt signaling and the evolution of embryonic posterior development. *Curr. Biol.* **19**, R215-R219.
McGregor, A. P., Pechmann, M., Schwager, E. E., Feitosa, N. M., Kruck, S., Aranda, M. and Damen, W. G. (2008). Wnt8 is required for growth-zone establishment and development of opisthosomal segments in a spider. *Curr. Biol.* **18**, 1619-1623.
McMahon, A., Reeves, G. T., Supatto, W. and Stathopoulos, A. (2010). Mesoderm migration in *Drosophila* is a multi-step process requiring FGF signaling and integrin activity. *Development* **137**, 2167-2175.
Milligan, G. (2004). G protein-coupled receptor dimerization: function and ligand pharmacology. *Mol. Pharmacol.* **66**, 1-7.
Miyawaki, K., Mito, T., Sarashina, I., Zhang, H., Shinmyo, Y., Ohuchi, H. and Noji, S. (2004). Involvement of Wingless/Armadillo signaling in the posterior sequential segmentation in the cricket, *Gryllus bimaculatus* (Orthoptera), as revealed by RNAi analysis. *Mech. Dev.* **121**, 119-130.
Ober, K. A. and Jockusch, E. L. (2006). The roles of *wingless* and *decapentaplegic* in axis and appendage development in the red flour beetle, *Tribolium castaneum*. *Dev. Biol.* **294**, 391-405.
Page, R. D. (1996). TreeView: an application to display phylogenetic trees on personal computers. *Comput. Appl. Biosci.* **12**, 357-358.
Patel, N. (1994). Imaging neuronal subsets and other cell types in whole-mount *Drosophila* embryos and larvae using antibody probes. *Methods Cell Biol.* **44**, 445-487.
Patel, N. H., Condron, B. G. and Zinn, K. (1994). Pair-rule expression patterns of *even-skipped* are found in both short- and long-germ beetles. *Nature* **367**, 429-434.
Pinson, K. I., Brennan, J., Monkley, S., Avery, B. J. and Skarnes, W. C. (2000). An LDL-receptor-related protein mediates Wnt signalling in mice. *Nature* **407**, 535-538.
Pueyo, J. I., Galindo, M. I., Bishop, S. A. and Couso, J. P. (2000). Proximal-distal leg development in *Drosophila* requires the *apterous* gene and the Lim1 homologue *dlim1*. *Development* **127**, 5391-5402.
Rulifson, E. J., Wu, C. H. and Nusse, R. (2000). Pathway specificity by the bifunctional receptor frizzled is determined by affinity for *wingless*. *Mol. Cell* **6**, 117-126.
Sambrook, J., Fritsch, E. F. and Maniatis, T. (1989). *Molecular Cloning-A Laboratory Manual*. Cold Spring Harbour Laboratory Press: Cold Spring Harbour, NY.
Schoppmeier, M. and Schröder, R. (2005). Maternal *torso* signaling controls body axis elongation in a short germ insect. *Curr. Biol.* **15**, 2131-2136.
Schröder, R., Beermann, A., Wittkopp, N. and Lutz, R. (2008). From development to biodiversity-*Tribolium castaneum*, an insect model organism for short germband development. *Dev. Genes Evol.* **218**, 119-126.
Schulte, G. and Bryja, V. (2007). The Frizzled family of unconventional G-protein-coupled receptors. *Trends Pharmacol. Sci.* **28**, 518-525.
Stiegler, A. L., Burden, S. J. and Hubbard, S. R. (2009). Crystal structure of the frizzled-like cysteine-rich domain of the receptor tyrosine kinase MuSK. *J. Mol. Biol.* **393**, 1-9.
Strimmer, K. and von Haeseler, A. (1996). Quartet puzzling: a quartet maximum likelihood method for reconstructing tree topologies. *Mol. Biol. Evol.* **13**, 964-969.
Tamai, K., Semenov, M., Kato, Y., Spokony, R., Liu, C., Katsuyama, Y., Hess, F., Saint-Jeannet, J. P. and He, X. (2000). LDL-receptor-related proteins in Wnt signal transduction. *Nature* **407**, 530-535.
Tautz, D. and Pfeifle, C. (1989). A non-radioactive in situ hybridization method for the localization of specific RNAs in *Drosophila* embryos reveals translational control of the segmentation gene *hunchback*. *Chromosoma* **98**, 81-85.
Tsuji, T., Sato, A., Hiratani, I., Taira, M., Saigo, K. and Kojima, T. (2000). Requirements of *Lim1*, a *Drosophila* LIM-homeobox gene, for normal leg and antennal development. *Development* **127**, 4315-4323.
Umbhauer, M., Djiane, A., Goisset, C., Penzo-Mendez, A., Riou, J. F., Boucaut, J. C. and Shi, D. L. (2000). The C-terminal cytoplasmic Lys-thr-X-X-X-Trp motif in frizzled receptors mediates Wnt/beta-catenin signalling. *EMBO J.* **19**, 4944-4954.
van Amerongen, R. and Nusse, R. (2009). Towards an integrated view of Wnt signaling in development. *Development* **136**, 3205-3214.
Van der Meer, J. M. (1977). Optical clean and permanent whole mount preparation for phase-contrast microscopy of cuticular sructures of insect larvae. *Drosophila Inf. Serv.* **52**, 160.
Wehrli, M., Dougan, S. T., Caldwell, K., O'Keefe, L., Schwartz, S., Vaizel-Ohayon, D., Schejter, E., Tomlinson, A. and DiNardo, S. (2000). *arrow* encodes an LDL-receptor-related protein essential for Wingless signalling. *Nature* **407**, 527-530.
Widelitz, R. (2005). Wnt signaling through canonical and non-canonical pathways: recent progress. *Growth Factors* **23**, 111-116.
Wu, J. and Mlodzik, M. (2008). The frizzled extracellular domain is a ligand for Van Gogh/Stbm during nonautonomous planar cell polarity signaling. *Dev. Cell* **15**, 462-469.
Wu, J., Klein, T. J. and Mlodzik, M. (2004). Subcellular localization of frizzled receptors, mediated by their cytoplasmic tails, regulates signaling pathway specificity. *PloS Biol.* **2**, E158.
Yamaguchi, T. P., Takada, S., Yoshikawa, Y., Wu, N. and McMahon, A. P. (1999). T (Brachyury) is a direct target of Wnt3a during paraxial mesoderm specification. *Genes Dev.* **13**, 3185-3190.
Yang-Snyder, J., Miller, J. R., Brown, J. D., Lai, C. J. and Moon, R. T. (1996). A *frizzled* homolog functions in a vertebrate *Wnt* signaling pathway. *Curr. Biol.* **6**, 1302-1306.

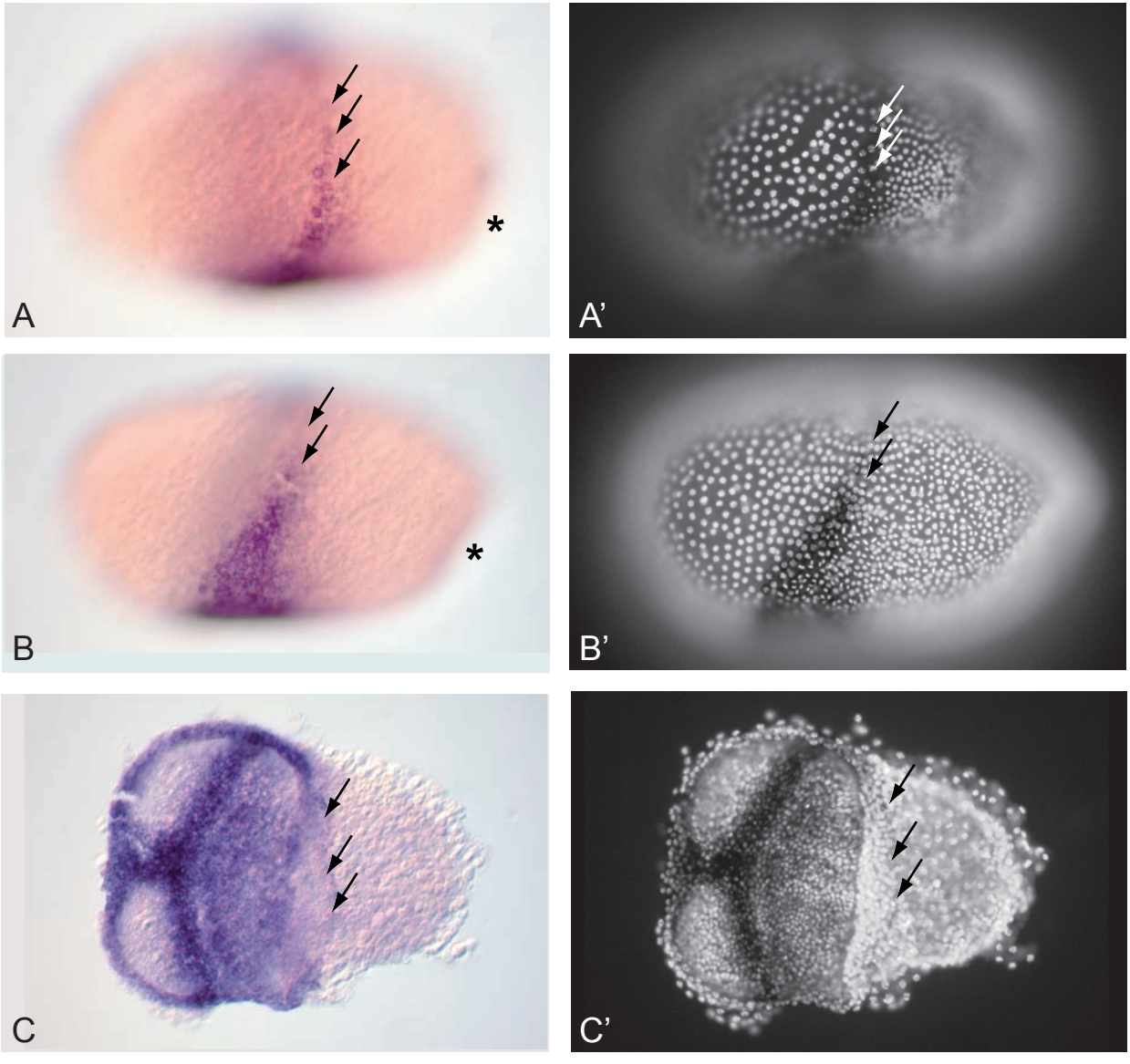
A
A'
B
B'
C
C'

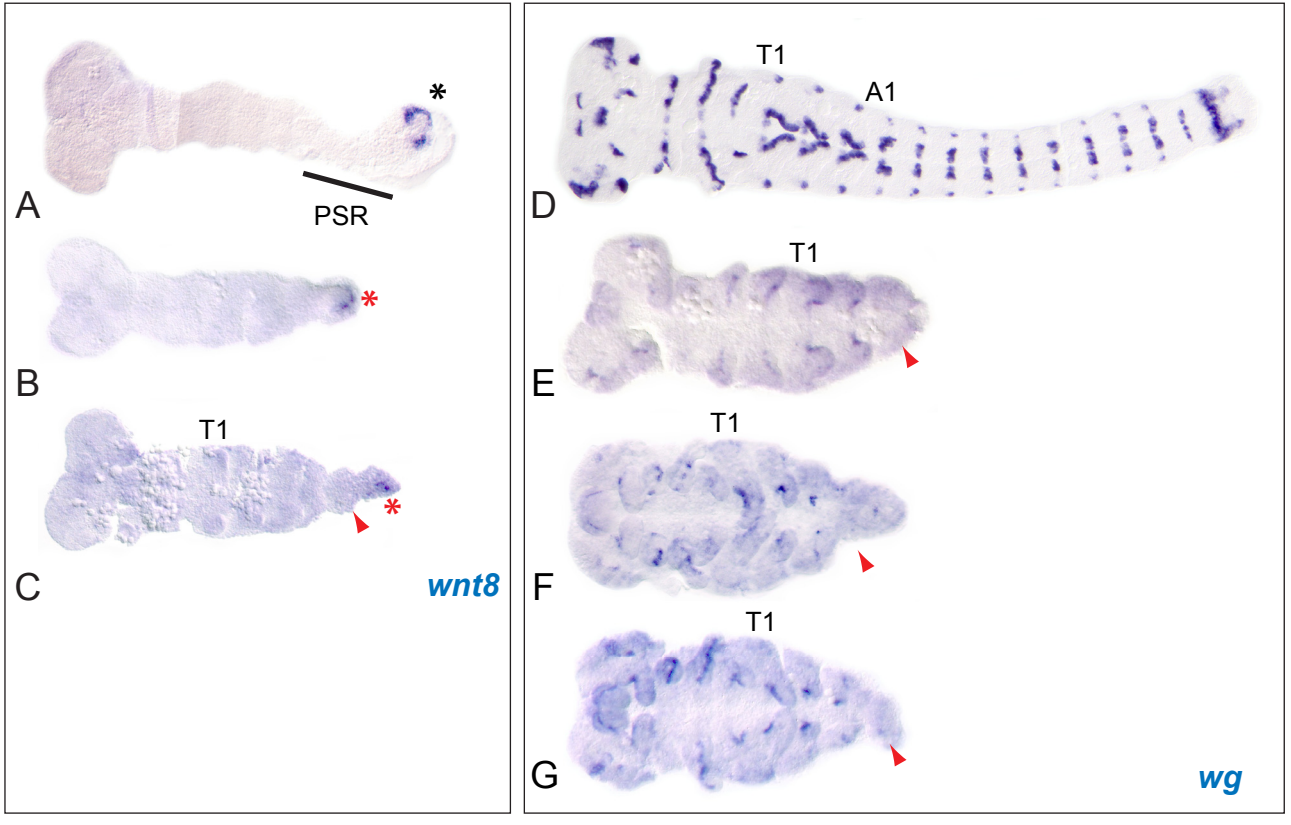
A
PSR
B
T1
C
wnt8
T1
A1
D
T1
E
T1
F
T1
G
wg

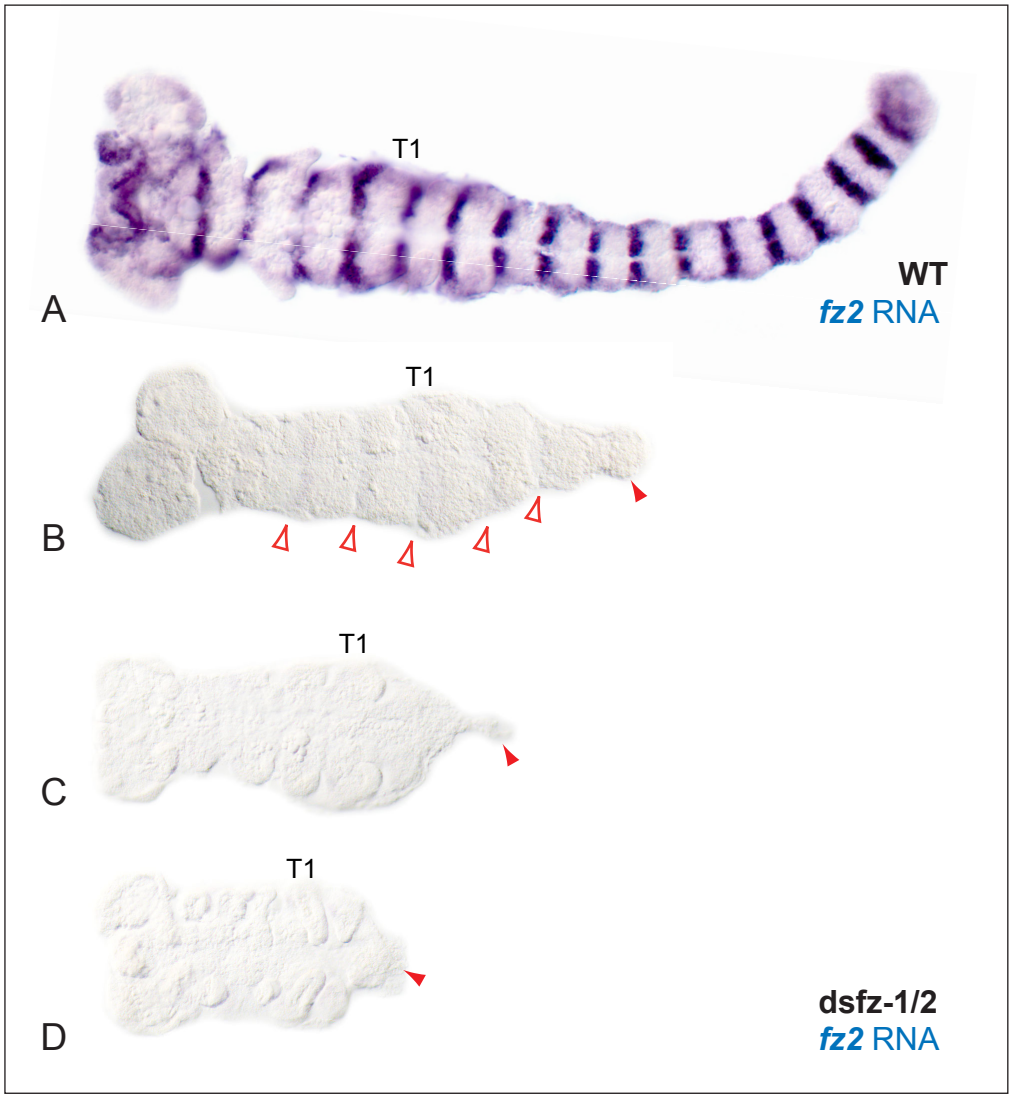
A
T1
WT
fz2 RNA
B
T1
C
T1
D
T1
dsfz-1/2
fz2 RNA

TM domain

5x the conserved PPP(S/T)Px(S/T) motif

```
Alignment Report of 'arrow-LRP alignTcDr#1497B14.meg' -  ClustalW (Slow/Accurate, Gonnet)

Trib.cast.   Arrow    KCKDGSCISLAHACDGIDHCADKSDEEACCR----DGFQCPNTQECLPANFVCDKIDHCADGSDEHPSHCNNASKLKVSSNGVVWIILGASGATMFISGI      1398
Dros.mel.    Arrow    SCQSGECIDKSLVCDGTTNCANGHDEADCCKR--PGEFQCPINKLCISAALLCDGWENCADGADESSDICLQRRMAPATDKRAFMILIGATMITIFSIVY      1468
Homo sap.    LRP5     PCARGQCVDLRLRCDGEADCQDRSDEADCDAICLPNQFRCAS-GQCVLIKQQCDSFPDCIDGSDELMCEITKPPSDDSPAHSSAIGPVIGIILSLFVMGG      1402
Homo sap.    LRP6     QCASGQCIDGALRCNGDANCQDKSDEKNCEVLCLIDQFRCAN-GQCIGKHKKCDHNVDCSDKSDELDCYPTEEP---APQATNTVGSVIGVIVTIFVSGT      1389

Trib.cast.   Arrow    LVYLLKRRS----SDDLNDQSEDSLS------------P--MQPKPHIKIRKGIPDVVRMSMMTG--SETSYDRNHITGASSS-TNESSLTCYPREPLNP      1477
Dros.mel.    Arrow    LLQFCRTRIGKSRTEPKDDQATDPLS------------PSTLSKSQRVSKIASVADAVRMSTLNSRNSMNSYDRNHITGASSSTTNGSSMVAYP---INP      1553
Homo sap.    LRP5     VYFVCQRVVCQRYAGANGPFPHEYVS-GTPHVPLNFIAPGGSQHGPFTGIACGKSMMSSVSLMGGRGGVPLYDRNHVTGASSSSSSSTKATLYP-PILNP      1500
Homo sap.    LRP6     VYFICQRMLCPRMKGDGETMTNDYVVHGPASVPLGYVPHPSSLSGSLPGMSRGKSMISSLSIMGGSSGPP-YDRAHVTGASSSSSSSTKGTYFP-AILNP      1487

Trib.cast.   Arrow    PPSPATTRGSS-------P--SSRYR--PYRHYRSINQPPPPTPCSTDVCDESDCNYPTRSR-----------------------YDAGPFPPPPTPRSH      1543
Dros.mel.    Arrow    PPSPATRSR----------------R--PYRHYKIINQPPPPTPCSTDICDESDSNYTSKSNSNNSNGGATKHSSSSAAACLQYGYDSEPYPPPPTPRSH      1635
Homo sap.    LRP5     PPSPATDPSLYNMDMFYSSNIPATAR--PYRPYIIRGMAPPTTPCSTDVCDS---DYSASR-------------WKASKYYLDLNSDSDPYPPPPTPHSQ      1582
Homo sap.    LRP6     PPSPATERSHYTMEFGYSSNSPSTHRSYSYRPYSYRHFAPPTTPCSTDVCDS---DYAPSRRMTSV--------ATAKGYTSDLNYDSEPVPPPPTPRSQ      1576

Trib.cast.   Arrow    CHS-------ESCPPSPSSRSSTYFNPLPPPPSPVASPPRGYDS                                                            1580
Dros.mel.    Arrow    YHSDVRIVPESSCPPSPSSRSSTYFSPLPPPPSPVQSPSRGFT                                                             1678
Homo sap.    LRP5     YLSAED-----SCPPSPATERSY-FHLFPPPPSPCTDSS                                                                 1615
Homo sap.    LRP6      YLSAEENY--ESCPPSPYTERSYSHHLYPPPPSPCTDSS                                                                  161
```

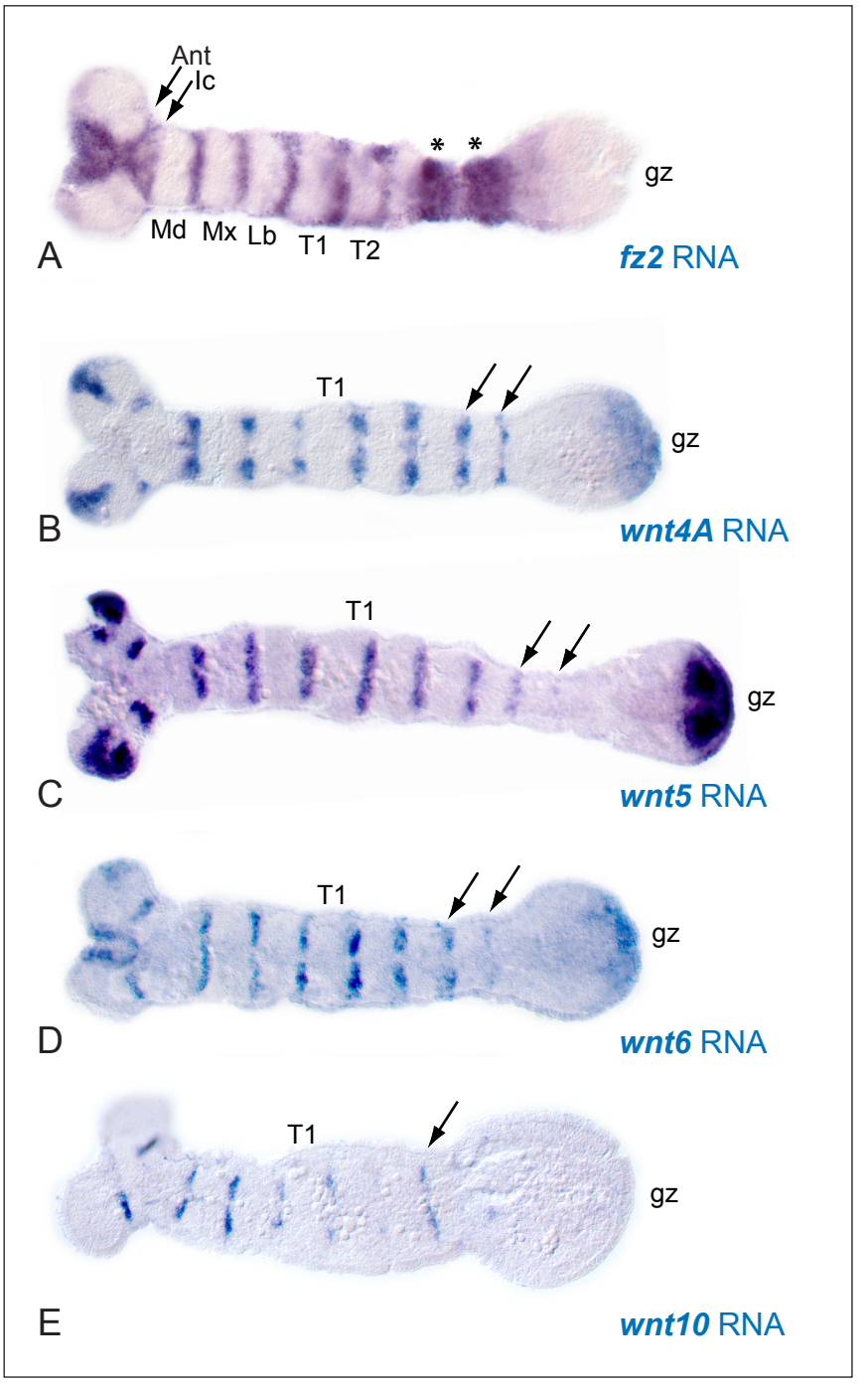
Ant
lc
* *
gz
Md Mx Lb T1 T2
A
fz2 RNA
T1
gz
B
wnt4A RNA
T1
gz
C
wnt5 RNA
T1
gz
D
wnt6 RNA
T1
gz
E
wnt10 RNA

Table S1. Larval cuticles: Numerical analysis of RNAi phenotypes

A. Summary. Pooled results originate from separate injection experiments using different dsRNA-concentrations (in red: concentrations used)

	Fz1/2 300 ng/µl / 1500 ng/µl	*Fz1* <1000 ng/µl / 1500 ng/µl	*Fz1/4*	*Fz4*	*arrow*	water
Total *n*	372 / 389	383 / 69	943	396	3290	130
Percentage of specific phenotypes (*n*)	72.5% (270) 43% (167)	29% (112) 29% (20)	57% (538)	2.5% (10)	10.5% (347)	– *
Percentage of empty eggs (*n*)	17.5% (65) 54.2% (211)	12% (45) 45% (31)	13% (121)	8.5% (34)	74% (2431)	6% (8)
Percentage of wild type (*n*)	10% (37) 2.8% (11)	59% (226) 26% (18)	30% (284)	89% (352)	15.5% (512)	94% (122)
Number of phenotypes =100%	270 / 167	112 / 20	538	10	347	–
Percentage of phenotypes classed as medium strength (*n*)	97% (262) 7.8% (13)	100% (112) 100% 20	98% (529)	50% (5)	43% (150)	–
Percentage of phenotypes classed as strong (spheres) (*n*)	3% (8) 92.2% (154)	–	2% (9)	50% (5)	57% (197)	–
Number of app.–/gut– phenotypes (*n*) =100%	–	112 / 20	529†	5	–	–
Percentage of app.– only phenotypes (*n*)	–	97% (109) 100% (20)	13% (67)	100% (5)	–	–
Percentage of app. and gut phenotypes (*n*)	–	3% (3) –	87% (462)	–	–	–

app., appendages.
*3% (*n*=4). Unspecific phenotype: flagellum of the antenna missing, but as this can be caused during the embedding procedure it is counted as wild type.
†For the comparison of fz1-fz1/4-fz4 RNAi, double stranded RNA of the same concentration was used in the single and the double RNAi experiments.

BRNAi experiments: injection series sorted by different dsRNA concentrations used

B1. Tc-fz1-RNA

	Fz1	*Fz1*	*Fz1*	*Fz1*
Concentration of dsRNA	300 ng/µl	650 ng/µl	1000 ng/µl	1500 ng/µl
Total *n* analysed cuticles	177	51	155	69
Percentage of specific phenotypes (*n*)	13.6% (24)	62.7% (51)	45.1% (70)	29% (20)
Percentage of empty eggs (*n*)	1.1% (2)	37.3% (19)	15.5% (24)	45% (31)
Percentage of wild type (*n*)	85.3% (151)	–	39.4% (61)	26% (18)
Number of phenotypes =100%	24	51	70	20
Percentage of phenotypes classed as medium strength (*n*)	100% (24)	100% (51)	100% (70)	100%
Percentage of phenotypes classed as strong (spheres) (*n*)	–	–	–	–
Number of app.–/gut– phenotypes (*n*) =100%	24	51	70	20
Percentage of app.– only phenotypes (n)	100% (24)	96% (49)	98.5% (69)	100% (20)
Percentage of app. and gut phenotypes (n)	–	4% (2)	1.5% (1)	–

B2. Tc-fz2 RNA

	fz2	*fz2*
Concentration of dsRNA	300 ng/µl	1500 ng/µl
Total *n* analysed cuticles	26	56
Percentage of empty eggs (*n*)	50% (13)	19.6% (11)
Percentage of wild type (*n*)	50% (13)	80.4% (45)

B3. Tc-fz1+Tc-fz2 double RNAi

	Fz1/2 (first injection series[‡])	*Fz1/2*	*Fz1/2*
Concentration of dsRNA	300 ng/µl	300 ng/µl	1500 ng/µl
Total *n* analysed cuticles	62	310	389
Percentage of specific phenotypes (*n*)	45.2% (28)	78% (242)	43% (167)
Percentage of empty eggs (*n*)	4.8% (3)	20% (62)	54.2% (211)
Percentage of wild type (*n*)	50% (31)	2% (6)	2.8% (11)
Number of phenotypes =100%	28	242	167
Percentage of phenotypes classed as medium strength (*n*)	93% (26)	97% (236)	7.8% (13)
Percentage of phenotypes classed as strong (spheres) (*n*)	7% (2)	3% (6)	92.2% (154)

[‡]This series was the first fz1/2 RNAi experiment performed by R.P.

B4. Tc-fz4-RNAi

	Fz4	*Fz4*	*Fz4*
Concentration of dsRNA	300 ng/µl	600 ng/µl	1000 ng/µl
Total *n* analysed cuticles	115	125	156
Percentage of specific phenotypes (*n*)	0.9% (1)	3.2% (4)	3.2% (5)
Percentage of empty eggs (*n*)	0.9% (1)	17.6% (22)	7% (11)
Percentage of wild type (*n*)	98.2% (113)	79.2% (99)	89.8% (140)
Number of phenotypes =100%	1	4	5
Percentage of phenotypes classed as medium strength (*n*)	100% (1)	25% (4)	60% (3)
Percentage of phenotypes classed as strong (spheres) (*n*)	–	75% (3)	40% (2)
Number of app.–/gut– phenotypes (*n*) =100%	1	1	3
Percentage of app.– only phenotypes (*n*)	100% (1)	100% (1)	100% (3)

B5. Fz1/4-double RNAi

	fz1/4	fz1/4	fz1/4	fz1/4
Concentration of dsRNA	300 ng/µl	650 ng/µl	650 ng/µl	1000 ng/µl
Total *n* analysed cuticles	180	245	257	261
Percentage of specific phenotypes (*n*)	66.1% (119)	78% (191)	82% (210)	7% (18)
Percentage of empty eggs (*n*)	0.6% (1)	21.6% (53)	14% (37)	11.5% (30)
Percentage of wild type (*n*)	33.3% (60)	0.4% (1)	4% (10)	81.5% (213)
Number of phenotypes =100%	119	191	210	18
Percentage of phenotypes classed as medium strength (*n*)	100% (119)	97% (185)	98.5% (207)	100% (18)
Percentage of phenotypes classed as strong (spheres) (*n*)	–	3% (6)	1.5% (3)	–
Number of app.–/gut– phenotypes (*n*) =100%	119	185	207	18
Percentage of app.– only phenotypes (*n*)	56.3% (67)	–	–	–
Percentage of app. and gut phenotypes (*n*)	43.7% (52)	100% (185)	100% (207)	100% (18)

B6. Tc-arrow RNAi

Concentration of dsRNA	10 ng/µl	50 ng/µl	100 ng/µl	300 ng/µl	600 ng/µl	600 ng/µl	1700 ng/µl
Total *n*	796	720	601	565	337	164	107
Percentage of specific phenotypes (*n*)	9.8% (78)	17.8% (128)	7.3% (44)	7.5% (43)	11.6% (39)	9.1% (15)	–
Percentage of empty eggs (*n*)	43.2% (344)	80% (576)	78.9% (474)	86.9% (491)	86.6% (292)	90.8% (149)	98.1% (105)
Percentage of wild type (*n*)	47% (374)	2.2% (16)	13.8% (83)	5.5% (31)	1.8% (6)	-	1.9% (2)
Number of phenotypes =100%	78	128	44	43	39	15	–
Percentage of phenotypes classed as medium strength (*n*)	53.8% (42)	37.5% (48)	36.4% (16)	30% (13)	30.7% (12)	26.6% (4)	–
Percentage of phenotypes classed as strong (spheres) (*n*)	46.2% (36)	62.5% (80)	63.6% (28)	70% (30)	69.3% (27)	73.3% (11)	–